"ROLE OF DIFFUSION-WEIGHTED MAGNETIC RESONANCE IMAGING IN THE EVALUATION OF RENAL MASSES: ONE YEAR HOSPITAL BASED OBSERVATIONAL STUDY"

BY

REG NO. BS0121002

Dissertation

Submitted to
KAHER, Belagavi, Karnataka,
In partial fulfilment of the requirements for the degree of

M.D.

In

RADIO-DIAGNOSIS

DEPARTMENT OF RADIO-DIAGNOSIS,
J. N. MEDICAL COLLEGE,
BELAGAVI -590010. KARNATAKA

DECEMBER - 2024

ENDORSEMENT CERTIFICATE

KLE ACADEMY OF HIGHER EDUCATION AND RESEARCH,

BELAGAVI, KARNATAKA

Endorsement by the HOD/Principal/ Head of the Institution

This is to certify that the dissertation entitled **"ROLE OF DIFFUSION-WEIGHTED MAGNETIC RESONANCE IMAGING IN THE EVALUATION OF RENAL MASSES: ONE YEAR HOSPITAL BASED OBSERVATIONAL STUDY"** is a bonafide research work done by **REG NO. BS0121002.**

Dr. SANTOSH D. PATIL
M.D.(Radio-Diagnosis)
Professor & HOD
Dept. of Radio-diagnasis
J.N. Medical College, BELAGAVI-10.
KMC Reg.No. 58456

Dr SANTOSH D. PATIL	**Dr N. S. MAHANTASHETTI**
M.D. RADIO-DIAGNOSIS	M. D. PEDIATRICS
Professor and Head,	Principal,
Department of Radio Diagnosis;	J. N. Medical College,
J. N. Medical College,	Nehru Nagar, Belagavi – 10
Nehru Nagar, Belagavi – 10	
Date: 26/06/2024	**Date :** 26/06/2024
Place: Belagavi	**Place : Belagavi**

UNDERTAKING

I, **Reg. No. BS0121002,** hereby declare that the information and the data mentioned in my dissertation entitled **"ROLE OF DIFFUSION-WEIGHTED MAGNETIC RESONANCE IMAGING IN THE EVALUATION OF RENAL MASSES: ONE YEAR HOSPITAL BASED OBSERVATIONAL STUDY"** belongs to me and is original. I am aware of the definition of plagiarism as detailed below:

- An act or instance of using or closely imitating the language and thoughts of another author without authorisation and the representation of that author's work as one's own, as by not crediting the original author.
- A piece of writing or other work reflecting such unauthorised use or imitation.
- The deliberate or reckless representation of another's words, thoughts or ideas as one's own without attribution in connection with the submission of academic work, whether graded or otherwise.

I hereby declare that the dissertation prepared by me is original one and does not involve plagiarism anywhere. In case at a later stage, it is found that I have indulged in plagiarism, then I am solely responsible for the same and the institution is at liberty to take any disciplinary action against me including cancellation of dissertation or any other penalties imposed by the University.

Date:

Place: Belagavi **(REG. NO. BS0121002)**

PLAGIARISM CERTIFICATE

KLE JAWAHARLAL NEHRU MEDICAL COLLEGE
(A constituent unit of KLE Academy of Higher Education & Research Deemed-to-be-University)
(Recognized by National Medical Commission, New Delhi)
Accredited 'A+' Grade by NAAC (3rd Cycle) Placed in Category 'A' by MoE (GoI)
Nehru Nagar, Belagavi- 590 010, Karnataka, INDIA
0831 - 2471350 0831 - 2470759 www.jnmc.edu incipal@jnmc.edu

Ref No: MDC/PG/ Date: 25-06-2024

"ACCEPTANCE LETTER"

The softcopy of thesis entitled: **"ROLE OF DIFFUSION-WEIGHTED MAGNETIC RESONANCE IMAGING IN THE EVALUATION OF RENAL MASSES: ONE YEAR HOSPITAL BASED OBSERVATIONAL STUDY"** has been submitted for anti-plagiarism check through Turnitin software. The scan has been carried out and the scanned output reveals a match percentage of **09%** which is within the acceptable limits of **10%** as per the guidelines given by UGC.

Guide.

KAHER BELAGAVI J. N. MEDICAL COLLEGE

Dr. (Mrs.) N.S. Mahantashetti.
Chairperson-Antiplagiarism Committee &
Principal,
J. N. Medical College, Belagavi.

To,
Reg. No. BS0121002
Postgraduate Student,
2021-22 Batch,
Department of Radio-Diagnosis
J. N. Medical College, Belagavi.

ETHICAL CLEARANCE CERTIFICATE

K.L.E. ACADEMY OF HIGHER EDUCATION AND RESEARCH
(Deemed – to- be- University)
Accredited 'A+' Grade by NAAC in (3rd Cycle) Placed in Category 'A' by MHRD (GoI)
JNMC INSTITUTIONAL ETHICS COMMITTEE
JAWAHARLAL NEHRU MEDICAL COLLEGE,
NEHRU NAGAR, BELAGAVI-590010 (KARNATAKA-INDIA)
Website: http//www.jnmc.edu
E-Mail : dome@jnmc.edu
Phone: (+ 91-(0)831 Office : 2472550
Principal: 2471701
Fax No. +91 (0)831 – 2470759

Ref No.MDC/JNMCIEC/ 51 **Date: 27/09/2022**

To,
REG NO. BS1021002
PG Student in Radiodiagnosis,
J. N. Medical College,
BELAGAVI.

Sub: Institutional Ethical Clearance for the study.

With reference to the above, we wish to inform you that your proposed research project titled **"ROLE OF DIFFUSION-WEIGHTED MAGNETIC RESONANCE IMAGING IN THE EVALUATION OF RENAL MASSES: ONE YEAR HOSPITAL BASED OBSERVATIONAL STUDY."** is ethical and justifiable. The proposed research project has been cleared by the JNMC Institutional Ethics Committee.

(Dr. Smita Sonoli)
Member Secretary
JNMC Institutional Ethics Committee
J.N.Medical College, Belagavi.

(Dr. Harsha Hegde)
Chairman,
JNMC Institutional Ethics Committee
J.N.Medical College, Belagavi

152

LIST OF ABBREVIATIONS

RCC	**Renal Cell Carcinoma**
CT	**Computed Tomography**
MRI	**Magnetic Resonance Imaging**
DWI	**Diffusion-Weighted Imaging**
ADC	**Apparent Diffusion Coefficient**
T1W	**T1 Weighted**
T2W	**T2 Weighted**
USG	**Ultrasonography**
ccRCC	**Clear Cell Renal Cell Carcinoma**
pRCC	**Papillary-Type Renal Cell Carcinoma**
chRCC	**Chromophobe-Type Renal Cell Carcinoma**
AML	**Angiomyolipoma**
CE MRI	**Contrast Enhanced Magnetic Resonance Imaging**
IR	**Inversion Recovery**
GFR	**Glomerular Filtration Rate**
SRM	**Small Renal Masses**
ROI	**Region of Interest**
FATSAT	**Fat Saturation**

TABLE OF CONTENTS

LIST OF FIGURES

LIST OF GRAPHS

LIST OF TABLES

ABSTRACT

BACKGROUND & OBJECTIVES: Diffusion-weighted imaging (DWI) utilises water molecule movement to assess tissue architecture, aiding in early metastasis detection, therapy response evaluation, and distinguishing between benign and malignant tumours in cancer imaging.

The main objective of this study is to evaluate the role of diffusion-weighted imaging in differentiating various subgroups of renal masses (i.e., viable solid tumours, necrotic or cystic tumours, and benign cysts).

MATERIALS AND METHODS: A one-year cross-sectional study was conducted in the department of radiodiagnosis at the KLES Dr. Prabhakar Kore Hospital and MRC, Belagavi. The total number of patients included in the study was 44. Patients from all age groups referred for a variety of clinical indications, including flank pain, hematuria, abdominal mass, and diagnosed & undiagnosed cases of renal carcinoma, etc., were considered.

These patients were subjected to MRI Abdomen imaging in a 3.0 Tesla Siemens MRI machine (Magnetom Spectra) in the Department of Radiology. The DWI sequence was added to the routine MRI protocol in all the patients undergoing MRI Abdomen imaging, and relevant findings were noted.

RESULTS: There were 23 and 21 patients, respectively, with benign lesions (36 cysts) and malignant lesions (eleven clear cell, two papillary, three chromophobe, one transitional cell carcinoma and five Wilms tumour). The malignant lesions were larger than the benign lesions (77.8 % of benign lesions <4 cm & 72.7% of malignant lesions >4 cm; $p = 0.011$, Chi-Square Test/Fisher Exact Test). The ADC values of the benign lesions were significantly higher than those of the malignant lesions (mean, 2.72 ± 0.078 vs $1.32 \pm 0.35 \times 10^{-3}$ mm^2/s; $p \leq 0.001$,

Student t Test). The ADCs of the 36 benign cysts were significantly higher than those of clear cell renal cancers (2.72 ± 0.078 vs 1.73 ± 0.42 × 10^{-3} mm^2/s; $p < 0.001$, Student t Test). There was a significant difference between the ADCs of clear and non–clear cell cancers (1.73 ± 0.42 vs 0.90 ± 0.29 × 10^{-3} mm^2/s; $p \leq 0.001$, Student t Test).

INTERPRETATION & CONCLUSION: Diffusion-weighted imaging (DWI) in renal MRI is a valuable technique for evaluating renal pathologies. It accurately distinguishes normal renal tissue from various disorders, especially when gadolinium use is contraindicated. DWI provides quantitative data and high-quality diagnostic images, enhancing its diagnostic utility.

In clinical practice, DWI aids in differentiating cystic benign lesions from cystic renal cell carcinoma, which is crucial for treatment decisions. It also helps categorise different subtypes of renal cell carcinoma, using ADC maps with specific b values like 0 and 800 s/mm^2 as biomarkers for histological subtyping.

Furthermore, DWI correlates with T1 signal characteristics of kidney lesions, providing additional diagnostic insights. Its non-invasive nature and ability to avoid contrast agent complications make it particularly advantageous in patient management. Overall, a DWI MRI of the kidney is integral in the comprehensive evaluation of renal masses, contributing significantly to accurate diagnosis and treatment planning in renal pathology.

KEYWORDS: Diffusion-weighted imaging, Apparent Diffusion Coefficient, magnetic resonance imaging, renal cell carcinoma, clear cell renal cell carcinoma, chromophobe type renal cell carcinoma, papillary type renal cell carcinoma, transitional cell carcinoma, Wilms tumour.

INTRODUCTION

In recent decades, the diagnosis of renal masses has witnessed a significant surge, primarily attributed to the widespread availability of CT and MRI. This increase in diagnosis is not just a statistical observation but a crucial development that can significantly impact the field of renal disease diagnosis and treatment. For instance, renal cell carcinoma (RCC) comprises about 3% of all adult cancers and represents approximately 85% of all kidney tumours[59]. While data from developed countries suggest that RCC typically occurs in individuals aged between their 6th and 7th decades of life, findings from India indicate that it affects people at a younger age [61,63]. Benign tumours comprise about 15-20% of all solid renal cortical tumours, with renal oncocytoma being the most common type [71].

Renal mass pathological diagnosis, aided by percutaneous biopsy[61], has challenges and risks. These include severe bleeding, harm to adjacent organs, tumour spreading, sampling errors that result in an underestimate of the tumour grade, and a significant non-diagnostic rate of 10–23%, frequently because of insufficient tissue samples. Furthermore, because of their proximity to essential blood arteries, predominantly cystic nature, tiny size, existence of a single kidney, obesity, or high risk of bleeding, some masses are not appropriate for biopsy. The distinction between benign or low-grade malignant tumours and high-grade malignant ones is sometimes unreliable when using conventional imaging techniques. For example, benign oncocytomas, minimal fat angiomyolipoma (AML), and RCCs can all have very similar features on CT scans and ultrasounds. These challenges and risks underscore the need for more reliable and less invasive diagnostic methods.

Because spontaneous motions like breathing, peristalsis, and blood flow are much more prominent than diffusional motion and may obscure the diffusion effect, diffusion-weighted imaging (DWI) in abdominal imaging has been restricted. Nevertheless, several motion-related issues may now be resolved, and reliable DWI pictures of the abdominal organs can be obtained because of recent developments in ultrafast MRI methods. DWI provides excellent opportunities for abdominal imaging, particularly in diffuse parenchymal disorders evaluation and localised lesion detection and characterisation where existing methods frequently fail.

Recent studies have already shown the promising potential of diffusion-weighted imaging (DWI) in evaluating various renal diseases, such as renal infection, renal ischemia, pyonephrosis, and diffuse renal disease [15, 31, 32, 34]. This emerging technology holds the key to more accurate and less invasive diagnosis, potentially revolutionising how we approach renal disease diagnosis and treatment.

REVIEW OF LITERATURE

DEFINITION:

WHAT IS DWI?

Diffusion-weighted imaging, a versatile tool, is based on the movement of water molecules and provides information about tissue architecture and integrity. It assists early metastasis detection, evaluates therapy response, and distinguishes benign from malignant tumours in cancer imaging. DWI can be used to assess liver fibrosis and characterise localised hepatic lesions in the liver, demonstrating its broad applicability [44]. It aids in the identification and localisation of prostate cancer in the prostate gland, and in identifying benign from malignant breast lesions and evaluating tumours' response to therapy.

Diffusion-weighted imaging has proven helpful in providing critical information for patient care and therapy decisions. However, its potential has yet to be fully realised. It is expected to evolve into an even more valuable tool for the early diagnosis and characterisation of a wide range of oncologic illnesses, promising a brighter future in medical imaging.

PRINCIPLES:

Diffusion-weighted imaging (DWI) in magnetic resonance imaging is based on the principle that water molecules move randomly within tissues. [18, 19, 20, 21]. Understanding free vs. restricted diffusion is crucial and fascinating, as it forms the basis for interpreting DWI results.[44]

Free water molecules demonstrate a random / Brownian motion, propelled by thermal kinetic energy, moving without hindrance. However, the water molecules within the

cell encounter obstacles from cellular compartments (cell walls, organelles) that impede their motion. The extent of this restricted diffusion directly reflects the tissue's cellularity, enlightening us on the intricate workings of the human body.

For instance, the diffusion of water molecules is curtailed in scenarios with an elevated number of cells with intact walls (as observed in malignancies, hypercellular metastases, or fibrosis). This restriction manifests as a decrease in signal intensity on DWI. Conversely, water molecules are more mobile in regions with a lower cell count or where cell membranes are compromised (such as the necrotic centre of a large mass), leading to less restricted diffusion and increased signal intensity on DWI.

Therefore, with its precise analysis of tissue characteristics based on the movement of water molecules, DWI offers invaluable insights for diagnosing and characterising a wide range of pathologies, instilling confidence in its clinical utility.

TECHNIQUE:

The Stejskal-Tanner sequence, a cornerstone in diffusion-weighted imaging, is the most widely used method[18, 19, 20]. This sequence, which skillfully integrates two symmetric motion-probing gradient pulses into an SSPE-weighted sequence, is based on the idea that a diffusion gradient causes a phase shift that changes with location. It's crucial to understand that during the two pulses of the sequence, spins that remain in the exact location (indicating a restricted diffusion microenvironment) along the gradient axis return to their initial state. However, spins that have migrated (which correspond to free water atoms) face an alternate field intensity during the second pulse. Hence, they cannot return to their starting state, resulting in a complete phase shift and a lower intensity of the observed MRI signal.

The degree of signal attenuation in diffusion-weighted imaging is influenced by a multitude of factors, as elucidated by the equation:

$SI = SI_0 \times \exp(-b \times D)$,

Where:

(SI) is the signal intensity with diffusion weighting applied.

(SI_0) is the signal intensity of the T2-weighted image with no diffusion gradient applied.

(b) is the degree of diffusion weighting (b value).

(D) is the diffusion coefficient.

The amplitude, duration, and temporal spacing of the two motion-probing gradients are increased to enhance the sensitivity of diffusion-weighted imaging to diffusion. In clinical practice, using multiple b values is not just a strategy but a prevalent and intriguing one. It's a method that reduces apparent diffusion coefficient (ADC) calculation errors, thereby enhancing tissue characterisation. The variation in b values allows for a more comprehensive assessment of tissue diffusion characteristics, underscoring their pivotal role in diffusion-weighted imaging.

QUANTITATIVE ANALYSIS WITH DIFFUSION-WEIGHTED IMAGING– ADC MAPPING:

The ADC (Apparent Diffusion Coefficient) is determined after processing using two b values in diffusion-weighted imaging. The ADC values reflect the slope of the line plotted on the graph showing the logarithm of signal intensity (y-axis) versus the b value (x-axis). Increasing the number of diffusion-weighted images with varying b values improves the precision of determining the ADC value.

The final image that shows ADC values calculated for each pixel is called an ADC map. One can determine the ADC value for an area by outlining areas within a lesion. Regions with diffusion and higher diffusion-weighted signals demonstrate ADC values.

It's important to consider that while ADC maps do not provide information, they should be examined alongside other MR images, such as diffusion-weighted images with different b values, high-resolution anatomical images, and possibly contrast-enhanced images. This thorough analysis ensures the interpretation of imaging results.

ARTIFACTS AND PITFALLS OF DIFFUSION-WEIGHTED IMAGING:

I. T2 SHINE-THROUGH EFFECT:

The spin-echo sequence used in DWI is T2-weighted, a complex process in which the T2 signal and the degree of signal attenuation after motion-probing gradient pulses are applied affect the tissue's signal intensity. The T2 shine-through effect, a nuanced phenomenon, occurs when a strong T2 signal in a tissue with a very long T2 relaxation period is misinterpreted for limited diffusion.

Making an ADC map is the simplest and most effective way to distinguish between T2 shine-through and true restricted diffusion. On the ADC map, restricted diffusion is represented by low signal intensity (low ADC values), whereas T2 shine-through is shown by high signal intensity. There are other additional techniques proven to be effective in reducing the T2 shine-through effect:

A. Using High b Value & Short Echo Time: A short echo time in conjunction with a high b value can effectively diminish the T2 signal, aiding in its differentiation from restricted diffusion.

B. Exponential Imaging Technique: Using an exponential function, DWI is divided by a non-weighted image to create a new image. By reducing the impact of the T2 signal, this technique helps distinguish between T2 shine-through and restricted diffusion more clearly.

II. MOTION ARTIFACT:

Motion artefact, a significant challenge in whole-body diffusion-weighted imaging studies, results from the continuous movement of various organs in the body. This artefact is prominent along the phase-encoding direction, leading to the formation of 'ghost' images. The signal generated is not limited to the particular original voxel but spreads across the entire image, potentially introducing errors in estimated ADC values. Understanding these challenges is crucial for devising effective strategies to overcome them.

To reduce this artefact, several strategies have been employed:

A. Increase Speed of Image Acquisition: Single-shot echoplanar imaging allows for faster image acquisition by reducing the time required to capture each image, enhancing image quality, and reducing the impact on ADC value estimation.

B. Utilize Parallel Imaging: Parallel imaging techniques exploit spatial information from multiple receiver coils to accelerate image acquisition, reducing the time required to acquire each image and decreasing susceptibility to motion artefacts.

In these methods, motion artefacts are reduced with accurate assessment & interpretation of ADC values.

III. EFFECT OF CONTRAST MATERIAL:

Performing whole-body DW imaging requires careful consideration of the impact of contrast material on the quantitative assessment of ADC values. This is significant in the renal parenchyma due to the high concentration of contrast material and the paramagnetic effects of contrast agents excreted into the collecting system.

In a study done by Wang et al. involving 50 patients, it was noted that the ADC signal of the renal parenchyma exhibited a significant decrease in post-contrast diffusion-weighted images. These post-contrast images were acquired approximately 11 minutes after the injection of contrast material. However, no substantial reduction in ADC values was noted after contrast material administration for the liver, pancreas, or spleen.

This finding underscores the importance of considering contrast material effects when interpreting ADC values, particularly in regions with high contrast agent concentration, such as the renal parenchyma. Such considerations are essential for accurate assessment and interpretation of whole-body diffusion-weighted imaging findings, ensuring reliable diagnosis and characterisation of pathology across various anatomical regions.

MRI ANATOMY OF KIDNEY:

The kidney's magnetic resonance imaging (MRI) anatomy offers a precise and detailed visualisation of the renal structures, including the renal parenchyma, collecting system, blood vessels, and surrounding tissues, instilling confidence in the accuracy of the information provided.

1. <u>Renal Parenchyma:</u>

- Cortex: The outer layer of the kidney, appearing as a hyperintense rim on T1-weighted images (which are suitable for anatomical detail) and a hypointense rim on T2-weighted images (which are ideal for fluid detection) (Figure 1.0).
- Medulla: The inner part of the kidney, consisting of renal pyramids separated by renal columns.
- Renal Pyramids: Triangular-shaped structures within the medulla, containing the renal tubules and collecting ducts.

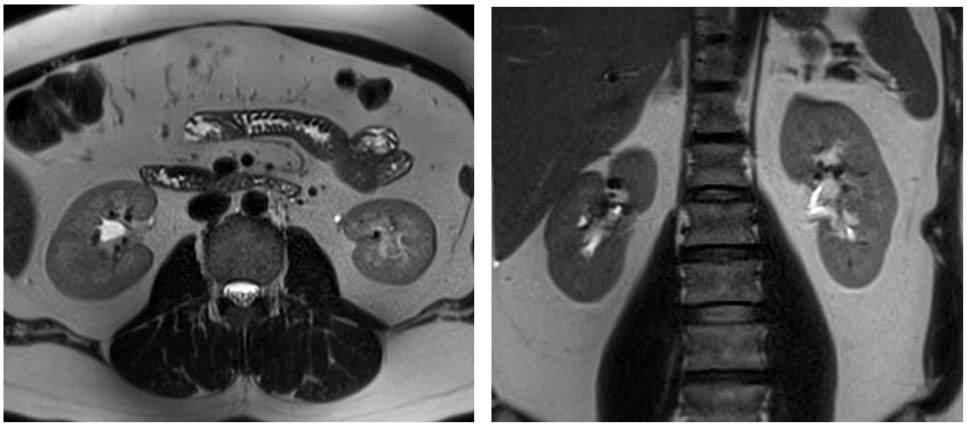

Figure 1 & 1.1: Axial & coronal T2W images of the normal kidneys show T2 hyperintense renal pyramids and T2 hypointense renal cortex.

2. <u>Renal Collecting System:</u>

- Renal Pelvis: The central region where urine collects before draining into the ureter (Figure 2).
- Calyces: Cup-shaped structure that collects urine from the renal pyramids and funnel it into the renal pelvis.

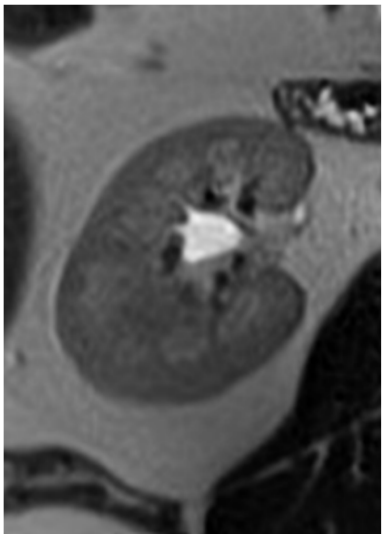

Figure 2: Axial T2W image of the right kidney shows an area of T2 high signal in the area of the renal sinus (the space within the kidney adjacent to the renal pelvis) suggestive of renal calyces.

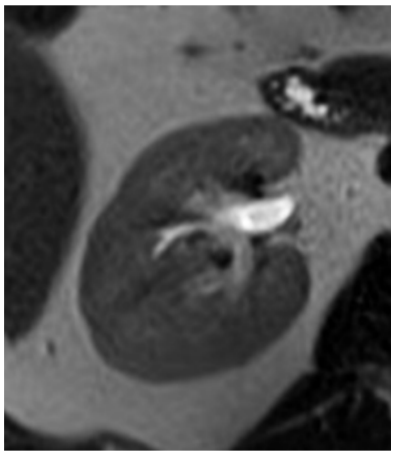

Figure 3: Axial T2W image of the right kidney shows an area of T2 high signal at the renal hilum suggestive of the renal pelvis

Renal vasculature:

- Renal Arteries and Veins: Supply and drain blood to and from the kidneys.
- Segmental Arteries: Branches of the renal artery supply blood to specific segments of the kidney (Figure 4).
- Interlobar Arteries and Veins: Run between the renal pyramids and supply and drain blood from the cortex.
- Arcuate Arteries and Veins: Arise from the interlobar vessels and arch over the base of the renal pyramids.
-

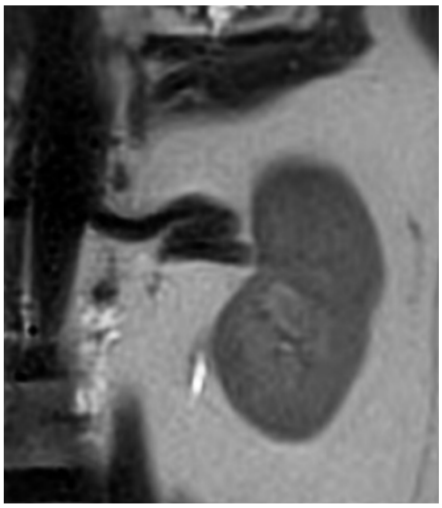

Figure 4: Coronal T2W image of the left kidney shows the main renal artery arising from the abdominal aorta and its segmental branch.

3. Surrounding Structures:

- Perirenal Fat: Surrounds the kidney and provides cushioning and protection.
- Gerota's Fascia: A layer of connective tissue that encapsulates the kidney and perirenal fat.
- Adrenal Glands: Sit atop each kidney and produce hormones such as cortisol and adrenaline.

THE BOSNIAK CLASSIFICATION SYSTEM:

The Bosniak classification system, a precise tool, categorises renal cystic lesions based on computed tomography (CT) or magnetic resonance imaging (MRI) findings [2,3]. It stratifies cystic renal masses based on their risk of malignancy, providing a confident guide for clinical management. [39, 40, 41]

1. Bosniak I: Simple Cysts

- Characteristics: Well-defined, thin-walled cysts with homogeneous fluid content and no enhancing components.
- Management: Typically, benign and requires no further evaluation or intervention.

2. Bosniak II: Minimally Complex Cysts

- Characteristics: Cysts with a few thin septations, minimally thickened or irregular walls, or a few non-enhancing mural nodules.

Management: Bosniak II cysts have a low risk of malignancy. However, follow-up imaging may be recommended to monitor for changes over time, ensuring early detection of potential issues.

1. Bosniak IIF: Indeterminate Cysts

- Characteristics: Cysts with more numerous or thicker septations, thicker irregular walls, or multiple enhancing mural nodules.
- Management: There is an intermediate risk of malignancy. Follow-up imaging or further evaluation with contrast-enhanced CT or MRI may be recommended.

2. Bosniak III: Suspicious Cysts

- Characteristics: Cysts with thickened irregular walls, multiple thick septations, or enhancing soft tissue components.
- Management: Moderate to high risk of malignancy. Surgical resection or biopsy may be considered for definitive diagnosis.

3. Bosniak IV: Overtly Malignant Cysts

- Characteristics: Cysts with enhancing solid components, nodularity, or cystic lesions with enhancing soft tissue masses.
- Management: High risk of malignancy. Surgical resection is often recommended for histological diagnosis and treatment.

The Bosniak classification provides a standardised framework for communication and ensures appropriate patient care. While the Bosniak classification system is widely used, it respects the importance of individual institutions or radiologists who may vary or modify the classification criteria based on their valuable clinical experience and available imaging modalities.

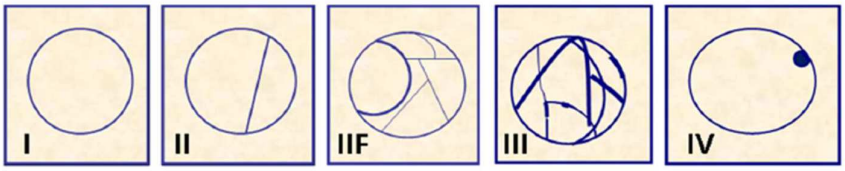

Bosniak stage	Risk of malignancy (%)	Features
I	0	Thin wall without septa or solid components. No internal enhancement.
II	0	Few (≤3) thin septa. It may show minimal enhancement of the septa. Hyperintense on T1 without enhancement.
IIF	5	Multiple (>3) thin septa. Smooth mild thickening (3 mm) of the wall or septa. It may contain minimal enhancement of the septa.
III	50	Thickened (>3 mm) wall or septa with enhancement. Irregular wall or septa with enhancement.
IV	90	Soft tissue enhancing mass independent from the wall.

Figure 5: Bosniak classification system for renal cystic lesions [(12)]

CHARACTERISATION OF SOLID RENAL MASSES:

CT and MRI are preferred over ultrasound (USG) due to their superior accuracy in detecting and characterising these masses. USG often misses small tumours and can show overlapping features between benign vs. malignant lesions.

The shape of solid renal masses provides a straightforward classification method. Nodular, well-defined masses cause a contour bulge, while infiltrative, ill-defined masses grow while maintaining the renal shape. This classification helps us understand the nature of the mass and guides us towards different diagnostic possibilities. For instance, nodular masses often raise concerns for malignancy, while infiltrative masses may indicate other pathological processes.

When a nodular mass without macroscopic fat is detected in the kidney, it is not just a finding but a potential indication of renal cell carcinoma (RCC). As the most common expansive solid masses in the kidney, RCCs are often incidentally detected when small (3 cm) and at an earlier stage. This early detection is not just a game-changer but a lifesaver, leading to a significantly better patient prognosis.

RCC is a condition with a wide range of histopathological entities, but three main subtypes dominate the landscape. Clear cell carcinoma (ccRCC) is the most prevalent, accounting for 80% to 90% of all RCCs. Unfortunately, ccRCC generally has a worse prognosis compared to other subtypes. On the other hand, there are also low-grade RCCs, which include papillary carcinoma (pRCC) and chromophobe carcinoma (chRCC). These subtypes are less common, accounting for 6–15% and 2– 5% of RCCs, respectively, but they tend to have better survival rates than ccRCCs, offering a glimmer of hope in the face of this challenging condition.

ANGIOMYOLIPOMA:

When a solid renal mass is detected, macroscopic (extracellular) fat is a sign and a significant indicator of angiomyolipoma (AML). This is because macroscopic fat in other renal masses, like renal cell carcinoma, is sporadic and typically associated with additional features like calcifications.

AMLs are tumours of mesenchymal origin that consist of varying proportions of blood vessels, smooth muscle cells, and adipocytes. They are not rare but relatively common in the general population, with prevalence ranging from 0.3% to 3%. There are two primary epidemiological forms: sporadic AML (which

constitutes 80% of cases and is most common in middle-aged women) and AML associated with tuberous sclerosis (20% of cases).

Confirming macroscopic fat in a renal mass is typically done using imaging techniques such as computed tomography or magnetic resonance imaging (MRI). In an MRI, the mass exhibits an iso-signal relative to subcutaneous or intraabdominal fat in all phases, including a Fat Saturation sequence.

It's crucial to reiterate that macroscopic fat is not just a feature but a key diagnostic feature for AML. While detecting signal drop (chemical shift) in an out-of-phase MRI sequence can indicate the presence of microscopic intracellular fat, this alone should not be relied upon for diagnosing AML, as many clear cell RCCs also contain fat. Therefore, macroscopic fat remains the definitive diagnostic feature for AML.

Tumor characterisation	**Clear cell RCC**	**Papillary RCC**	**Chromophobe type RCC**
T2W signal	High to intermediate	Low	Intermediate
In-phase/Out-phase	Out-phase signal drop due to microscopic fat	In-phase signal loss due to hemosiderin deposition	Homogeneous
Enhancement	++++	+	++
Necrosis	+++	Absent/ small cystic changes	Absent

Table 1: MRI imaging characterisation of clear cell renal cell carcinoma(ccRCC), papillary type renal cell carcinoma (pRCC) & chromophobe type renal cell carcinoma (chRCC).

Diffusion-weighted imaging (DWI) is valuable for characterising solid masses, particularly in renal lesions. Here's how it can be helpful:

1. Apparent Diffusion Coefficient (ADC) Values:

- ADC values obtained from DWI reflect the diffusion of water molecules within tissues. Higher ADC values indicate greater diffusion and can suggest specific tissue characteristics.

Recent meta-analyses have highlighted significantly higher ADC values in oncocytomas than RCC. This distinction can help differentiate between these two types of renal masses.

Additionally, studies have observed significant differences in ADC values between different subtypes of RCCs. For instance, the papillary subtype exhibits lower ADC values than other RCC subtypes.

2. Clinical Application:

- The differences in ADC values between oncocytomas, RCC subtypes, and other renal masses, as revealed by DWI, can practically assist radiologists and clinicians in making more accurate diagnosis, enhancing the value of this imaging technique in your daily practice.

When combined with other imaging modalities and clinical data, DWI comprehensively evaluates solid renal masses. This comprehensive approach guides treatment decisions and prognostic assessments, underscoring the breadth of DWI's usefulness in your clinical setting.

In conclusion, integrating DWI into the imaging protocol offers significant advantages in understanding the diffusion properties of tissues. Higher ADC values are typically observed in oncocytomas; variations exist among different RCC subtypes. This integration not only enhances the characterisation of solid renal masses but also enhances diagnostic precision.

REVIEW OF PREVIOUS STUDIES:

1. The retrospective study of Kumaresan Sandrasegaran et al. in 2009 at Indianapolis aimed to evaluate the utility of DWI in distinguishing between various subgroups of renal masses. The study measured the apparent diffusion coefficients (ADCs) of renal masses, where malignant lesions are proved through biopsy/ surgical pathology and benign cystic lesions demonstrate stability without treatment for a minimum follow-up period of 24 months. The study comprised twenty patients with benign lesions and 22 patients with malignant lesions.

   The results revealed that the ADC values of benign lesions were statistically higher than malignant lesions. Moreover, ADC measurements proved helpful in histologic subtyping of RCC. This underscores the potential of DWI in improving diagnostic accuracy and its relevance in guiding treatment decisions, particularly in patients for whom gadolinium-based contrast agents are contraindicated. [6]

2. The retrospective study conducted by Hynek Mirka et al. in Prague in 2015 involved 143 tumours in 139 patients, comprising 130 malignant tumours and 13 benign tumours. The tumors were examined using diffusion-weighted imaging (DWI) with b values of 50, 400, and 800 s/mm². These b values represent the strength of the

diffusion-sensitizing gradients used in the DWI sequence, with higher values indicating stronger gradients and more sensitive detection of diffusion.

Their findings underscore the precision of DWI in renal tumour characterisation and grading, suggesting that assessing the diffusion of water molecules in renal tumours using apparent diffusion coefficient (ADC) measurements may aid in distinguishing clear cell renal cell carcinoma (CCRCC) from other histological variants of renal carcinomas and determining its grade. This practical application of DWI could potentially enhance the precision of treatment planning. Additionally, the method demonstrated the potential for differentiating between benign and malignant tumours, particularly between the most typical representatives, oncocytoma and ccRCC grade I. [4]

3. The retrospective study by Jingbo Zhang, MD, et al. in New York in 2007 aimed to evaluate the utility of ADCs for characterising various renal masses. The study included 25 patients (fifteen men, ten women) aged 39 to 75 years with renal diseases and tumour types. All patients underwent renal magnetic resonance (MR) imaging, including diffusion-weighted imaging, before nephrectomy.

   Among the 25 individuals, 26 kidney tumours were discovered. Eleven benign cysts were found in eight individuals. Renal tumours had lower ADCs (median, 189.3 x 10^{-5} mm^2/s; range, [102.0-262.0] x 10^{-5} mm^2/s compared with benign cysts (median, 322.8 x 10^{-5} mm^2/s; range, [217.0-421.0] x 10^{-5} mm^2/s; $P <$ .001). Solid-enhancing tumours had significantly lower ADCs (median, 162.3 x 10^{-5} mm^2/s; range, [102.0-284.0] x 10^{-5} mm^2/s) compared with non-enhancing necrotic or cystic regions (median, 247.7 x 10^{-5} mm^2/s; range, [85.2-310.0] x 10^{-5} mm^2/s; $P = .007$).

Their findings suggested a correlation between the T1 signal characteristics of a renal lesion and its ADC. This implies that ADC measurements may offer valuable insights into characterising and differentiating renal masses, including viable solid tumours, necrotic or cystic tumour areas, and benign cysts. These insights can potentially guide treatment decisions, such as the choice between surgery and conservative management, and improve patient outcomes. [5]

4. In 2004, M. Cova, MD et al. conducted a study in Italy that involved 39 participants, including ten regular volunteers and 29 patients with known renal lesions. The participants underwent an MRI of the kidneys using a 1.5 Tesla superconducting magnet.

   Their findings indicated that the renal diffusion-weighted magnetic resonance imaging (DW MRI) is feasible and reliable for differentiating between normal renal parenchyma and various renal diseases. Notably, the acquisition time for the DW sequence was only 17 seconds, allowing for the rapid acquisition of diagnostic-quality DW images and quantitative data on diffusivity. This study highlights the potential clinical utility of DW MRI in renal imaging, offering both qualitative and quantitative information about renal tissue characteristics while also emphasising its efficiency in the diagnostic process. [1]

5. The retrospective study conducted by Suresh de Silva et al. in 2021 in England aimed to evaluate the utility of MRI imaging, specifically diffusion-weighted imaging (DWI) with apparent diffusion coefficient (ADC) characteristics, in assessing renal masses. The study included all patients who underwent MRI imaging for renal masses at the same imaging facility between June 2014 and June 2019.

Of the 66 patients examined for ADC characteristics, the distribution of renal masses was as follows: 33 (50.0%) Clear Cell RCC, 11 (16.7%) Oncocytoma, 9 (13.6%) Angiomyolipoma, 9 (13.6%) Papillary Type 1 RCC, and 4 (6.1%) Chromophobe RCC.

The study's results suggested that renal MRI DWI/ADC imaging holds promise in differentiating oncocytomas and angiomyolipoma from RCCs. Additionally, it may assist in stratifying RCC subtypes, particularly in challenging cases where biopsy or surgery may pose a high risk or be infeasible. [7]

6. The retrospective study conducted by Bachir Taouli, MD et al. in 2009 in New York aimed to compare the diagnostic performance of diffusion-weighted (DW) magnetic resonance (MR) imaging with contrast-enhanced (CE) MR imaging and assess the combined performance of these examinations for the characterisation of renal lesions. MR follow-up and histopathologic analysis served as the reference standards.

   The study included 109 renal lesions in 64 patients (46 men and 18 women) with a mean age of 60.7 years. These lesions were evaluated using CE MR imaging and breath-hold DW imaging with various b values.

   The findings suggested that DW imaging can be utilised to characterise renal lesions. However, it was found to be less accurate compared to CE MR imaging. Despite this, DW imaging demonstrated utility in differentiating solid renal cell carcinomas (RCCs) from oncocytomas and characterising the histologic subtypes of RCC. The combination of DW and CE MR imaging may provide complementary information, potentially enhancing the overall diagnostic performance for renal lesion characterisation. These findings have important implications for

clinical practice, suggesting that combining imaging modalities may be more effective in characterising renal lesions than using a single modality alone. [8]

7. In 2004, Israel GM et al. studied cystic renal masses using CT and MR imaging and compared their effectiveness based on the Bosniak classification system.

   The Bosniak classification system categorises cystic renal masses based on their imaging features, helping to guide management decisions. The study compared the performance of CT and MR imaging in utilising this classification system.

   The study's findings, published in RSNA, demonstrated that CT and MR imaging effectively evaluated cystic renal masses using the Bosniak classification system. However, the study did not indicate a superiority of one modality over the other. Instead, it highlighted the complementary roles of CT and MR imaging in assessing cystic renal masses. [9]

8. Carbone SF et al. conducted a preliminary study in 2007 to investigate the utility of diffusion-weighted magnetic resonance imaging in assessing renal function. The study, published in Radiologia Medica, aimed to evaluate the potential of DW-MRI as a tool for renal function assessment.

   Fourteen patients (nine men and five women, mean age 49 years, range 22-66 years) underwent an MR examination on a 1.5-T system. The glomerular filtration rate (GFR) assessed by Cockcroft-Gault's equation was used as a functional marker. ADC was 2.44+/-0.24 x 10^{-3} mm^2/s in patients with normal GFR and 2.05+/-0.33 x 10^{-3} mm^2/s in subjects with altered GFR; a significant difference was found between stage III and IV, whereas no differences were found between stage I and II and between stage II and III. A good correlation was found between GFR and ADC, with no significant change after furosemide administration. [10]

9. The study conducted by Thoeny et al. in 2005 explored the utility of diffusion-weighted magnetic resonance imaging (DW-MRI) in assessing kidney health in both healthy individuals and patients with renal parenchymal diseases. This research, published in RSNA, aimed to provide early insights into the application of DW-MRI in renal imaging.

Eighteen healthy volunteers and 15 patients participated in the study. The study calculated various apparent diffusion coefficient (ADC) values to discern the impact of perfusion and diffusion. These included the ADC of all b values (ADC (avg)), the ADC of low b values (b = 0, 50, 100 sec/mm²; ADC (low)), and the ADC of high b values (b = 500, 750, 1000 sec/mm²; ADC (high).

The results showed that in healthy volunteers, ADC (average) and ADC (high) were significantly higher in the cortex compared to the medulla ($P < .001$). However, no difference between the cortex and medulla was observed for ADC (low). In patients with renal failure, ADC values for both cortex and medulla were significantly lower compared to volunteers ($P < .001$, $P = .004$ for ADC (avg); $P = .02$, $P = .03$ for ADC (low); $P = .02$, $P = .04$ for ADC (high). All ADC values in pyelonephritis were significantly lower than the contralateral side. Still, individuals with ureteral blockage showed varied differences in all ADC values compared to the contralateral side.

The study found no statistically significant changes in the repeat study of the volunteers.

The study concluded that DW MR imaging is feasible and reproducible in evaluating renal function based on the initial experience with a few patients and

volunteers. This suggests the potential for DW-MRI to contribute to the assessment of renal health and pathology. [11]

10. In 2004, the study by Squillaci E et al. aimed to investigate the correlation between diffusion-weighted magnetic resonance imaging (DW-MRI) findings and the cellularity of renal tumours. Published in Anticancer Research, this study provided insights into the potential of DW-MRI in assessing the cellular characteristics of renal tumours.

    Twenty healthy volunteers and 18 patients with renal tumours were enrolled in this study. The DWI sequence was performed before contrast administration utilising a single-shot SE EPI Inversion Recovery (IR) procedure.

    The early findings suggest renal tumours have a lower mean apparent diffusion coefficient (ADC) value than normal kidney tissue. Surprisingly, the ADC value of tumours didn't seem significantly linked to how densely packed the tumour cells were. Still, it showed a connection to the overall structure of the tumour, as seen under the microscope.

    These early findings hint at the potential of using diffusion-weighted imaging (DWI) to quickly gather crucial information about the composition of kidney tumours, all within a short 17-second scan. This could potentially revolutionise clinical practice, offering doctors a non-invasive way to understand the makeup of these tumours without the need for invasive procedures. [13]

11. The 2008 study by Sasaki M et al. aimed to assess the variability in absolute apparent diffusion coefficient (ADC) values across different MRI platforms. Published in RSNA, this study conducted a multivendor, multi-institutional comparison to evaluate the consistency of ADC measurements obtained from different MRI scanners.

Diffusion-weighted (DW) images with nearly identical parameters were obtained at 1.5 and 3.0 T from 12 healthy volunteers at seven institutions using ten magnetic resonance (MR) images provided by four vendors. ADC maps were created from isotropic DW maps, and pictures with b value of 0 sec/mm^2 were created. The absolute ADC values of grey and white matter from the same vendor differed substantially: 4%-9% at 1.5 and 3.0 T. Except for one vendor, the intervendor variability at 1.5 T was as high as 7%. Moreover, there was substantial intra-imager variability, up to 8%, depending on the coil systems in certain imagers.

The significant variability in ADC values based on the coil systems, imaging machines, manufacturers, and magnetic field strengths used in MRI scans suggests a potential solution, as indicated by this study. The use of relative ADC values, rather than absolute ones, might be more appropriate for assessing diffusion abnormalities in patients participating in multicenter trials for acute ischemic stroke.[14]

12. Namimoto T et al. conducted a study published in the Journal of Magnetic Resonance Imaging in 1999. The study aimed to measure diffuse renal disease's ADC using diffusion-weighted echo-planar imaging.

Diffuse renal diseases, a complex range of conditions affecting the entire kidney parenchyma, such as acute and chronic renal parenchymal diseases, nephritis, and fibrosis, have been the focus of our research. The ADC, derived from DW-EPI, provides a comprehensive understanding of the diffusion characteristics of water molecules within renal tissues, offering deep insights into tissue microstructure and pathophysiology.

The study likely involved imaging a cohort of patients with diffuse renal disease using DW-EPI sequences. ADC measurements were obtained from regions of interest within the renal parenchyma and compared between patients with different types and stages of renal disease.

The study's findings likely demonstrated alterations in renal ADC values associated with diffuse renal diseases. Changes in ADC may reflect differences in tissue cellularity, fibrosis, inflammation, or oedema within the renal parenchyma, providing valuable information for diagnosing and monitoring renal disease progression. Overall, this study likely contributed to our understanding of the role of DW-EPI and ADC mapping in assessing diffuse renal diseases and provided insights into the potential utility of these techniques in clinical practice for evaluating renal function and pathology. [58]

13. In their study published in the Journal of the Belgian Radiological Society (JBR-BTR) in 2002, Verswijvel G, Vandecaveye V, Gelin G, Vandevenne J, Grieten M, Horvath M, et al. investigated the utility of diffusion-weighted magnetic resonance imaging (DW-MRI) in the evaluation of renal infection.

Renal infection, such as pyelonephritis, can lead to inflammatory changes within the renal parenchyma. DW-MRI measures the diffusion of water molecules within tissues, which can be sensitive to changes in tissue microstructure and cellularity associated with inflammation.

The study likely involved imaging a cohort of patients with suspected renal infection using DW-MRI sequences. By analysing the DW-MRI findings, including apparent diffusion coefficient (ADC) values and signal intensity

characteristics, the researchers aimed to assess the diagnostic utility of DW-MRI in detecting and characterising renal infection.

The study's findings likely demonstrated the potential of DW-MRI as a noninvasive imaging technique for evaluating renal infection. DW-MRI may offer additional insights into the extent and severity of inflammatory changes within the renal parenchyma, aiding in diagnosing and managing renal infections.

Overall, this study likely provided preliminary evidence supporting the use of DW-MRI in assessing renal infection. [33]

14. In a 1994 study published in Radiology, Muller MF, Prasad PV, Bimmler D, Kaiser A, and Edelman RR investigated functional imaging of the kidney by measuring the apparent diffusion coefficient (ADC). This study provided valuable insights into the potential of DW-MRI in functional imaging of the kidney.

The study likely involved using diffusion-weighted magnetic resonance imaging (DW-MRI) techniques to measure the ADC in the kidneys of a cohort of patients. By acquiring DW-MRI images and calculating ADC values, the researchers aimed to noninvasively assess renal function and integrity.

The apparent diffusion coefficient reflects the diffusion rate of water molecules within tissues, providing insights into tissue microstructure and function. ADC values may indicate changes in tissue cellularity, fibrosis, or inflammation within the kidney parenchyma.

The study findings likely demonstrated alterations in renal ADC values associated with various renal pathologies, such as acute kidney injury, chronic kidney disease, or renal masses. By correlating ADC measurements with clinical data and

renal function tests, the study likely provided insights into the functional significance of ADC changes in renal disease. [28]

15. In a 1995 study published in the Journal of Magnetic Resonance Imaging, Siegel CL, Aisen AM, Ellis JH, Londy F, and Chenevert TL explored the feasibility of conducting magnetic resonance (MR) diffusion studies in the kidney.

    The study likely involved imaging a cohort of patients or volunteers using DW-MRI sequences specifically tailored for renal imaging. The researchers likely assessed the quality of DW-MRI images obtained from the kidneys. They evaluated the feasibility of quantifying diffusion parameters within renal tissues, such as the apparent diffusion coefficient (ADC).

    The study's findings likely demonstrated the technical feasibility of performing DW-MRI studies in the kidney. Despite the challenges posed by respiratory and cardiac motion, the researchers likely showed that DW-MRI could yield informative images of renal anatomy and potentially provide valuable insights into renal function and pathology. Overall, this study laid the groundwork for subsequent research on DW-MRI in renal imaging. It highlighted its potential as a non-invasive imaging modality for assessing renal physiology and pathology. [17]

16. In their 2018 study published in the International Urology and Nephrology journal, Mytsyk et al. examined the utility of the apparent diffusion coefficient (ADC) obtained from diffusion-weighted magnetic resonance imaging (DW-MRI) in distinguishing small renal masses (SRM).

    The study involved 158 adult patients with 170 SRMs, compared to a control group of 15 healthy volunteers with typical clinical and radiological findings. All participants underwent MRI with DWI sequences.

The findings revealed that the mean ADC values of solid renal cell carcinoma were significantly lower (1.65 ± 0.38 × 10-3 mm^2/s) than those of healthy renal parenchyma (2.47 ± 0.12 × 10-3 mm^2/s, $p < 0.05$). However, no significant difference was observed in mean ADC values among clear cell RCC, papillary RCC, and chromophobe RCC. An inverse correlation was noted between mean ADC values and the Fuhrman grade of nuclear atypia of solid ccRCCs.

Furthermore, significant differences were observed in mean ADC values between solid RCCs, benign renal tumours, and renal cysts (1.65 ± 0.38 × 10-3 vs 2.23 ± 0.18 × 10-3 vs 3.15 ± 0.51 × 10-3 mm^2/s, respectively), as well as between benign cysts and cystic RCC. [22]

AIMS & OBJECTIVES

The study aimed to evaluate the role of diffusion-weighted imaging in differentiating various subgroups of renal masses. (i.e., viable solid tumours, necrotic or cystic tumours, & benign cysts).

MATERIALS AND METHODS

From 1 January 2023 to 31 December 2023, patients were referred for a MRI Abdomen with DWI for clinically suspected renal masses to the department of Radiodiagnosis at The KLE's Dr Prabhakar Kore Hospital & MRC, Belgaum, Karnataka, India.

Study Design: Hospital-based observational cross-sectional study

Study Period: One year – between January 2023 to December 2023

Sample Size:

The minimum sample size formula based on the prevalence rate is

$$n = \frac{z_\alpha^2 \, P(1- P)}{d^2}$$

P is the percentage of prevalence, and d is the percentage of likely difference in prevalence.

$z\alpha$ is linked with the level of significance. For a 5% level of significance, $z\alpha = 1.96$.

Ref:

With P = 30% and d = 25% of P = 7.50%, the sample size is 44.

Sampling technique: Universal Random Sampling

Inclusion Criteria:

- Patients referred with a variety of clinical indications, including flank pain, hematuria, abdominal mass, and diagnosed and undiagnosed cases of renal carcinoma.
- Patients from all age groups will be included in the study.

Exclusion Criteria:

- Contraindications to MRI.
- Patients with metallic medical implants (intraocular metallic foreign body, cardiac pacemakers, MR non-compatible intracranial clips of arterial brain aneurysms).
- Patients who refused to do the examination.

Study protocol:

Institutional Ethical Clearance from the Institutional Ethics Committee from Human Subject Research of Jawaharlal Nehru Medical College, Belagavi, Karnataka, was obtained. All patients coming to the institution during the study period with complaints of renal masses were advised for Magnetic Resonance Imaging-Diffusion Weighted Imaging. Patients fulfilling all the inclusion criteria and none of the exclusion criteria and willing to provide voluntary consent for participation in the study were enrolled. Forty-four patients with renal masses were included for statistical significance.

Data collection procedure:

The study followed a systematic approach, using a 3.0 Tesla Siemens MRI machine (Magnetom Spectra). A standard scan protocol was meticulously applied to all the patients with renal pathology undergoing DWI MRI Sequence. Their DWI sequence was thoroughly evaluated, and the Apparent Diffusion Coefficient (ADC) values were calculated monoexponentially with all 'b' value sequences using the scanner software. Four and six oval regions of interest (ROIs) were precisely placed over the renal masses on the ADC maps. These ROIs included a large one encompassing as much of the mass as possible but excluding normal kidneys. The minimum value of the mean ADC measurements of all the ROIs was used for

analysis and denoted as the minimum ADC for the lesion. In cases where there are multiple masses in a kidney, the ADCs of the most significant two masses, measuring more than 1.5 cm, were obtained.

MRI SEQUENCES THAT WILL BE OBTAINED:

- Diffusion-weighted imaging
- Axial and Sagittal T1-weighted dual-echo in-phase and out-of-phase sequences
- Axial and Coronal T2-weighted single-shot fast spin-echo sequences
- Axial - T1 FATSAT

Figure 6: 3.0 Tesla Siemens MRI machine (Magnetom Spectra).

Data processing and analysis/statistical analysis:

Since the study was observational, the analysis plan was as follows.

For the continuous quantitative variables, mean and standard deviation were calculated. If the data was divided into two groups concerning specific qualitative characteristics, the continuous variables were compared using suitable statistical tools, like the student's unpaired t-test. The pre-and post-treatment measures were compared using the student's paired t-test.

A median represents discrete variables. The categorical data will be expressed in rates, ratios, and percentages. The association between the outcome and clinical and demographic characteristics was tested using the Chi-square test, a test of proportion, or Fisher's exact test. Nonparametric tests were used for discrete variables. Apart from the above, suitable tools like ANOVA, correlation, regression, etc., were used as needed. Suitable graphs were used to depict the comparison.

The p-value of less than 5% (0.05) was considered significant for all the tests.

OBSERVATION & RESULTS

TABLE 2: AGE IN YEARS-FREQUENCY DISTRIBUTION OF PATIENTS STUDIED

Age in Years	No. of Patients	%
1-10	4	9.1
11-20	1	2.3
21-30	1	2.3
31-40	4	9.1
41-50	6	13.6
51-60	15	34.1
61-70	9	20.5
>70	4	9.1
Total	44	100.0
Mean	49.68	
SD	19.40	

In this study population, the mean age was 49.68±19.40 years.

Among the study population, 4 (9.1 %) cases were aged 1-10 years, 1 (2.3 %) case was aged between 11-20 years, 1 (2.3 %) case was aged 21-30 years, 4 (9.1 %) cases were aged between 31-40 years, 6 (13.6 %) cases were between 41-50 years, 15 (34.1 %) cases aged between 51-60 years, 9 (20.5 %) cases aged between 61-70 years and 4 (9.1 %) cases aged more than or equal to 71 years.

GRAPH 1: AGE IN YEARS-FREQUENCY DISTRIBUTION OF PATIENTS STUDIED

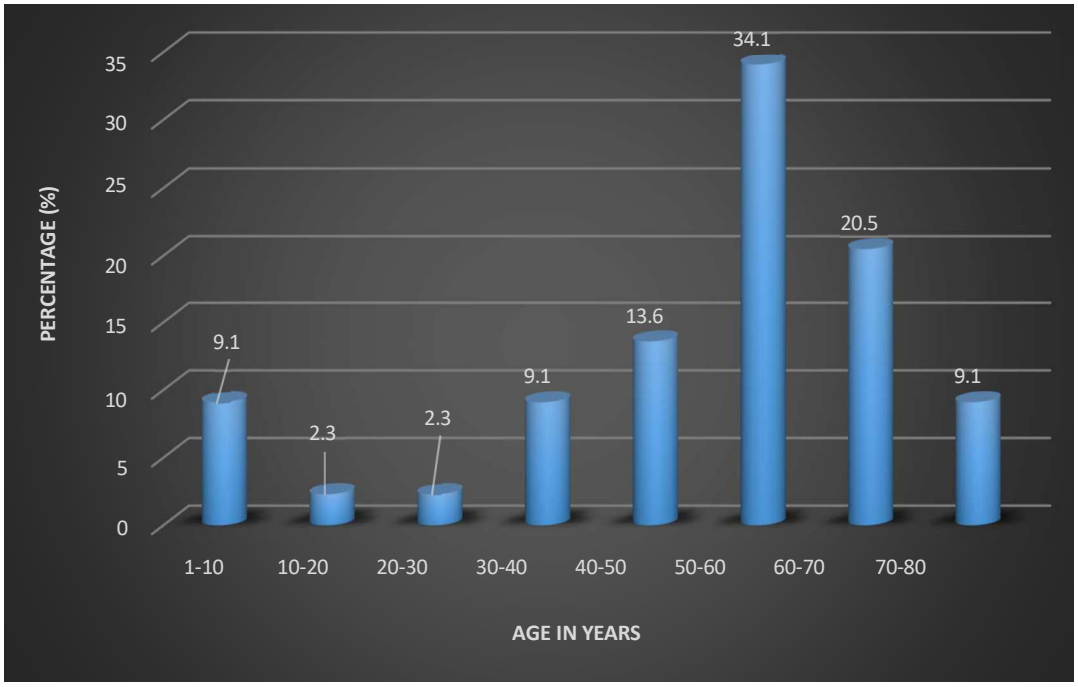

TABLE 3: GENDER- FREQUENCY DISTRIBUTION OF PATIENTS STUDIED

Gender	No. of Patients	%
Female	17	38.6
Male	27	61.4
Total	44	100.0

Among the study population, 27 (61.4 %) were males and the remaining 17 (38.6 %) were females.

GRAPH 2: GENDER- FREQUENCY DISTRIBUTION OF PATIENTS STUDIED

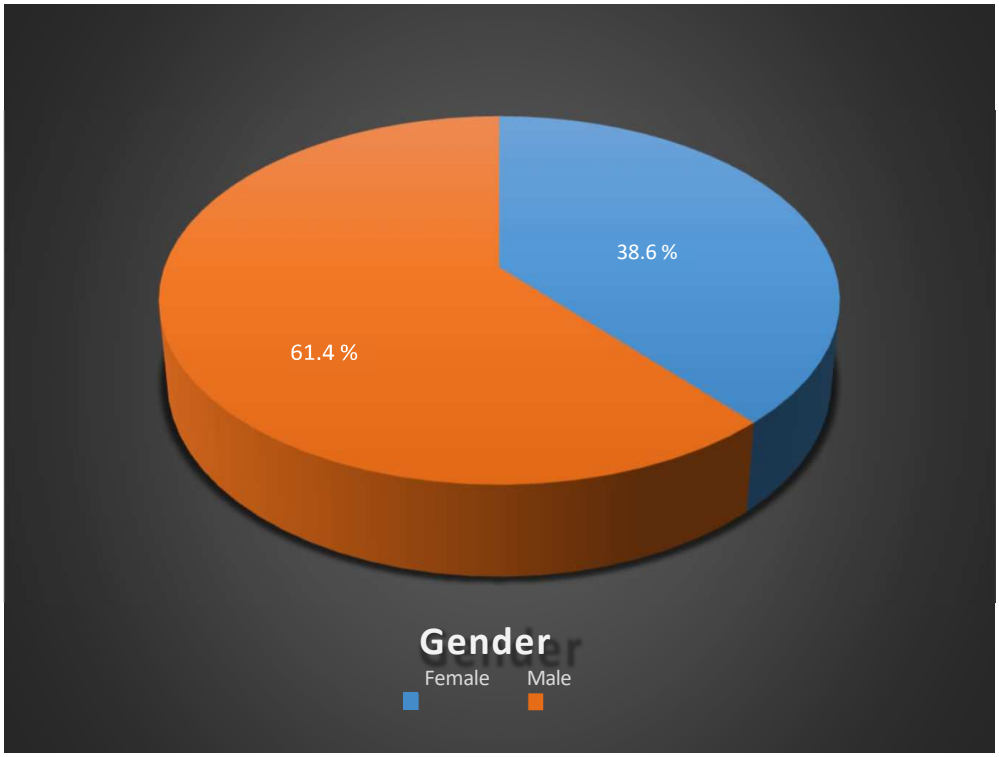

TABLE 4: SYMPTOMS- FREQUENCY DISTRIBUTION OF PATIENTS STUDIED

SYMPTOMS	No. of Patients	%
No	11	25.0
Yes	33	75.0
• ABDOMINAL PAIN	27	61.4
• HEMATURIA	13	29.5
• BURNING MICTURITION	10	22.7
• WEIGHT LOSS	10	22.7
• LOSS OF APPETITE	9	20.5
• ABDOMINAL DISTENSION	4	9.1
• URINARY INCONTINENCE	4	9.1
• NAUSEA	1	2.3
• VOMITING	1	2.3
Total	44	

Among the study population, 25% of the patients (11 cases) had no symptoms, and the remaining 75% (33 cases) presented with various symptoms. The most common symptom was abdominal pain (61.4%), followed by hematuria (29.5%) and burning micturition (22.7%). The least common symptoms were nausea and vomiting (each with 2.3%).

GRAPH 3.1: SYMPTOMS- PRESENT OR ABSENT

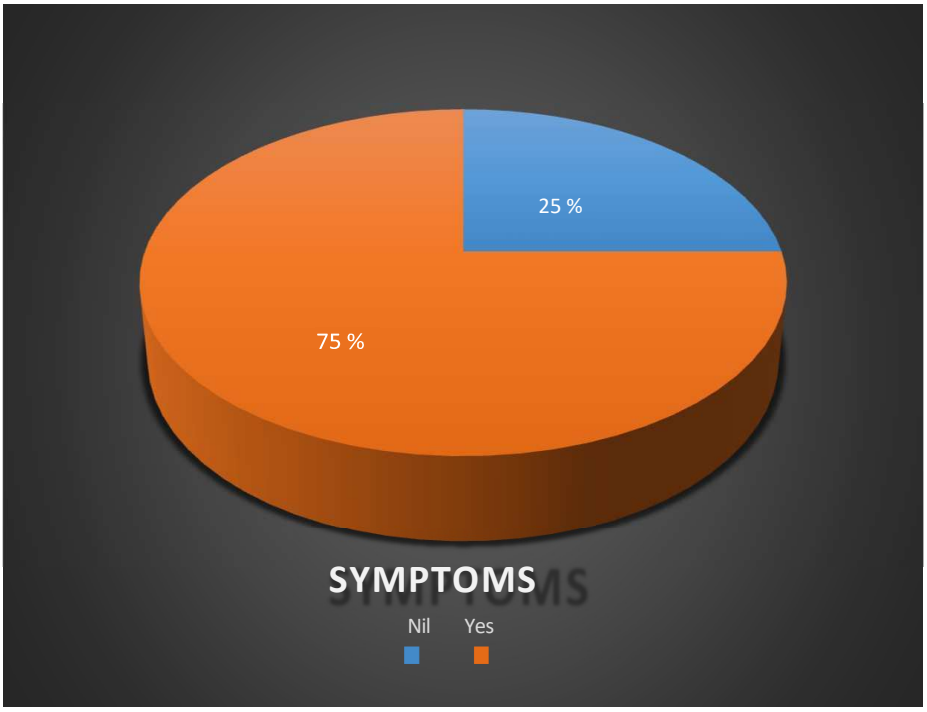

GRAPH 3.2: SYMPTOMS- FREQUENCY DISTRIBUTION OF PATIENTS STUDIED

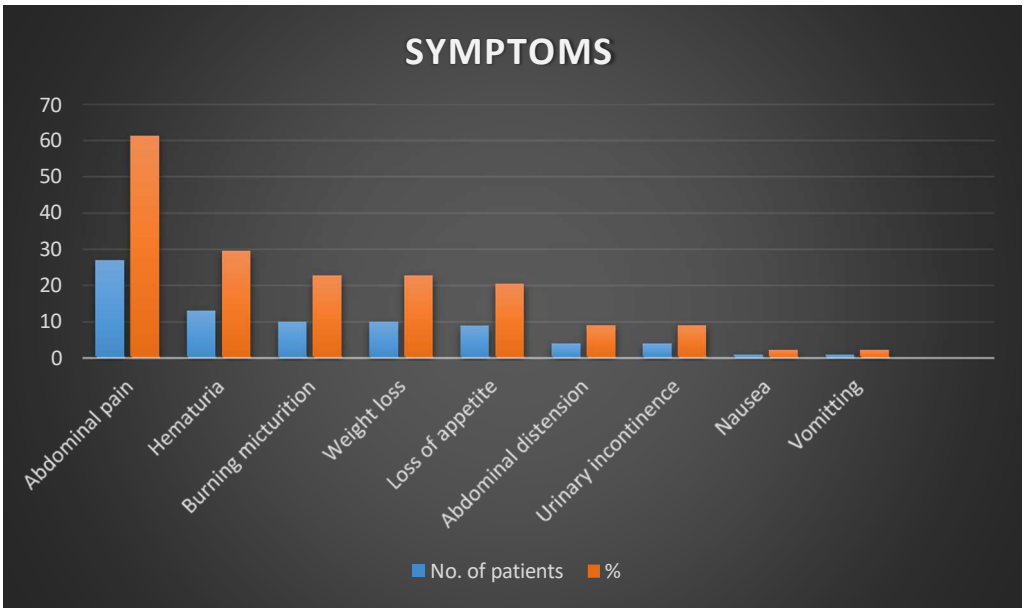

TABLE 5: CO-MORBIDITIES- FREQUENCY DISTRIBUTION OF PATIENTS STUDIED

CO-MORBIDITIES	No. of Patients	%
Absent	14	31.8
Present	30	68.2
Total	44	100.0

Among the study population, 14 patients (31.8%) had no co-morbidities, and 30 (68.2%) had various comorbidities.

GRAPH 4: CO-MORBIDITIES- FREQUENCY DISTRIBUTION OF PATIENTS STUDIED

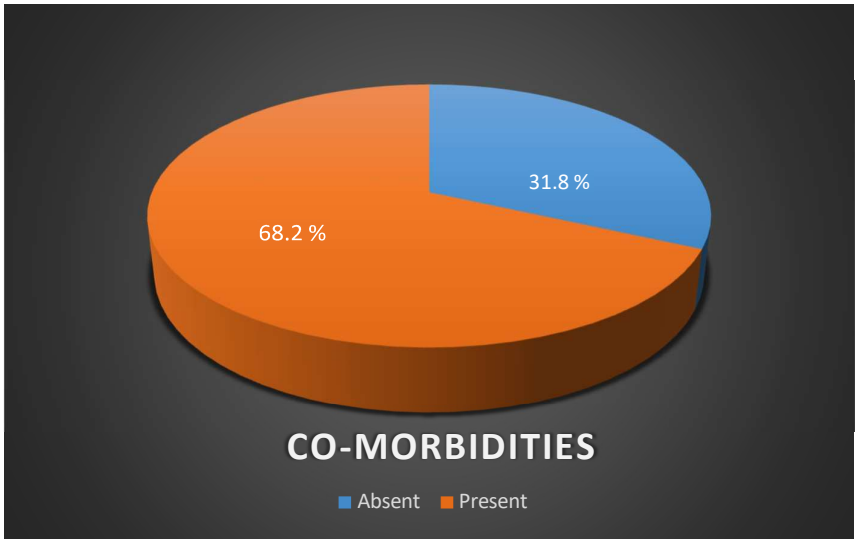

TABLE 6: SIDE AFFECTED- FREQUENCY DISTRIBUTION OF PATIENTS AFFECTED

SIDE AFFECTED	No. of Patients	%
Both	7	15.9
Left Side	18	40.9
Right Side	19	43.2
Total	44	100.0

There was no significant difference among the study population regarding the side of the kidney affected. The right side was affected in 19 cases (43.2%), the left side was affected in 18 cases (40.9%), and both sides were affected in 7 cases (15.9%).

GRAPH 5: SIDE AFFECTED- FREQUENCY DISTRIBUTION OF PATIENTS STUDIED

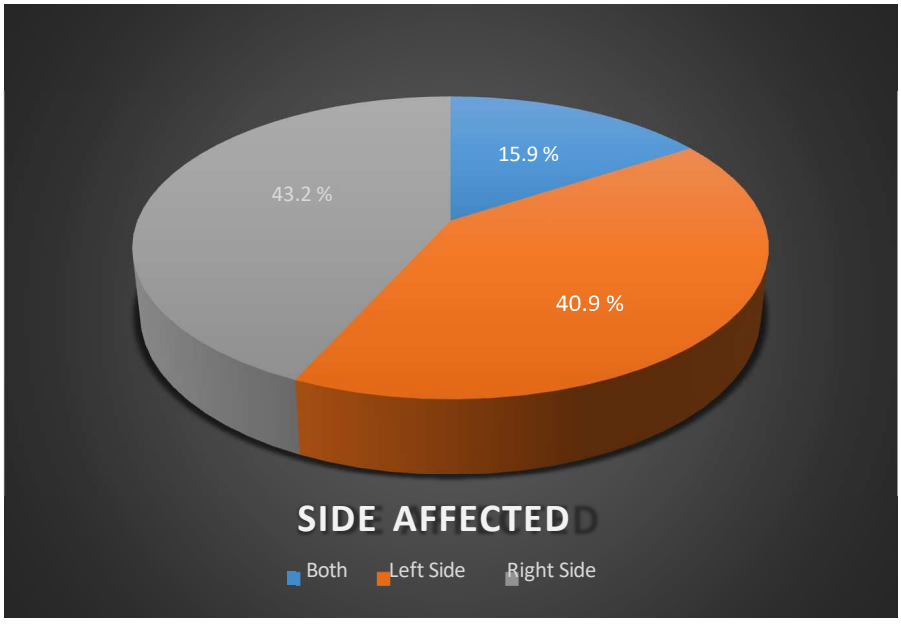

TABLE 7: SIZE (CM)- FREQUENCY DISTRIBUTION OF LESIONS STUDIED

Variables	**No. of Lesions (n=58)**	**%**
size <4cm	34	58.6
size 4-8 cm	15	25.9
size >8 cm	9	15.5

Among the lesions studied, most (58.6%) were less than 4 cm in size, 15 lesions (25.9%) were between 4 and 8 cm in diameter, and a few (15.5%) were more than 8 cm in diameter.

GRAPH 6: SIZE (CM)- FREQUENCY DISTRIBUTION OF LESIONS STUDIED

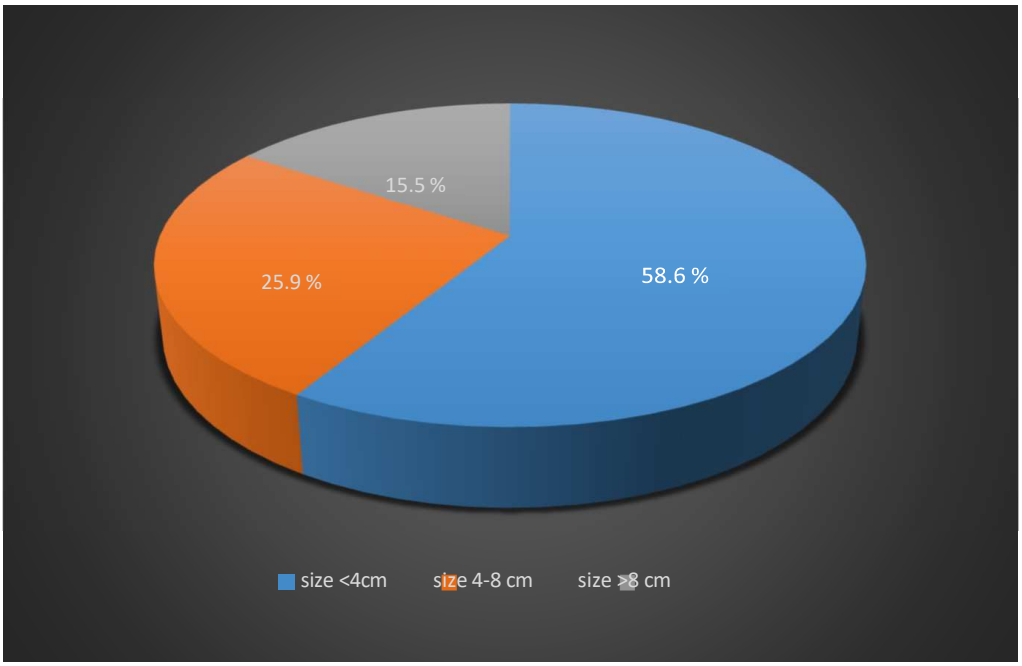

TABLE 8: TYPE OF LESION- FREQUENCY DISTRIBUTION OF LESIONS STUDIED

Variables	No. of Lesions (n=58)	%
SOLID LESION	22	36.2
CYSTIC LESION	34	58.6
COMPLEX CYSTIC LESION	2	3.4

Out of 58 lesions under evaluation, 34 cystic lesions were seen (58.6%), followed by 22 solid lesions (36.2%), with the least being two complex cystic lesions (3.4%).

GRAPH 7: LESIONS- FREQUENCY DISTRIBUTION OF LESIONS STUDIED

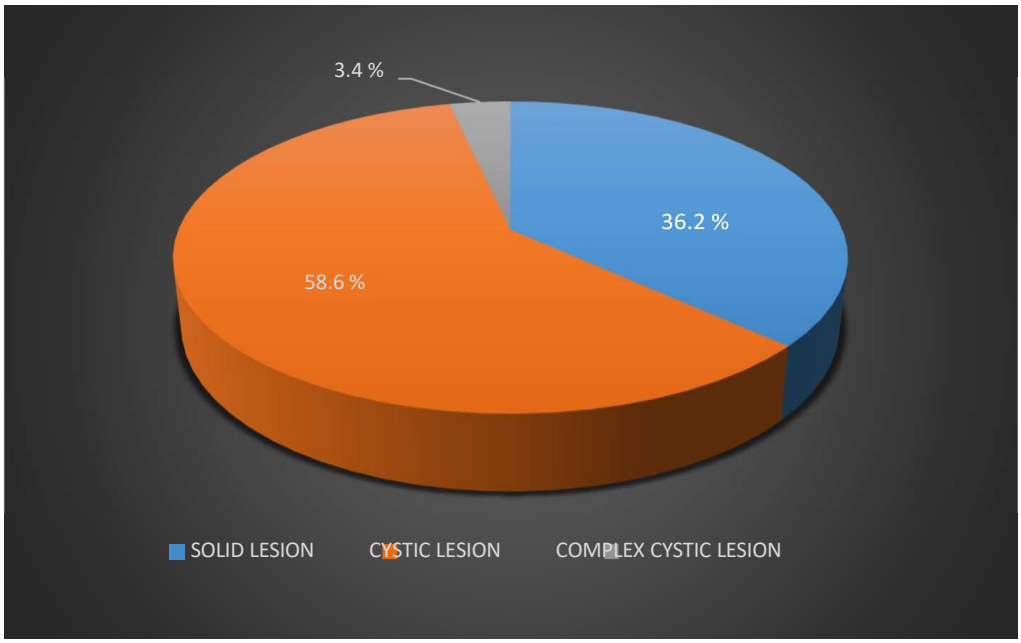

TABLE 9: T1W/ T2W- FREQUENCY DISTRIBUTION OF LESIONS STUDIED

Variables	**No. of Lesions (n=58)**	**%**
T1W		
• HYPERINTENSE	3	5.2
• HYPOINTENSE	46	79.3
• HYPOINTENSE TO ISOINTENSE	2	3.4
• ISOINTENSE	7	12.1
T2W		
• HYPERINTENSE	43	74.1
• HYPOINTENSE	3	5.2
• ISOINTENSE TO HYPERINTENSE	7	12.1
• ISOINTENSE	5	8.6

Among the lesions studied, the most common signal intensity seen in T1W imaging is 'hypointense' (79.3%), noted in 46 lesions, and the most common signal intensity seen in T2W imaging is 'hyperintense' (74.1%), indicated in 43 lesions.

GRAPH 8.1: T1W - FREQUENCY DISTRIBUTION OF LESIONS STUDIED

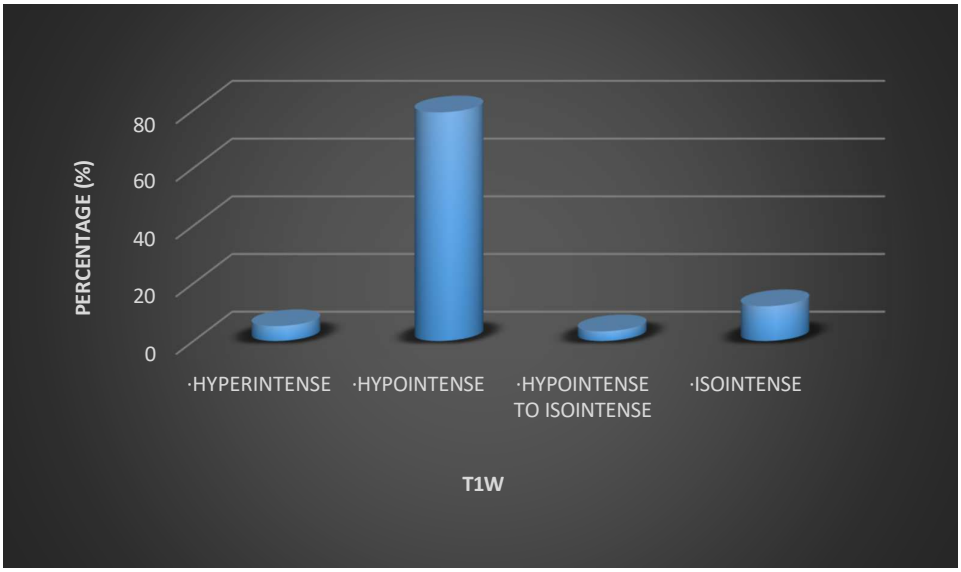

GRAPH 8.2: T2W - FREQUENCY DISTRIBUTION OF LESIONS STUDIED

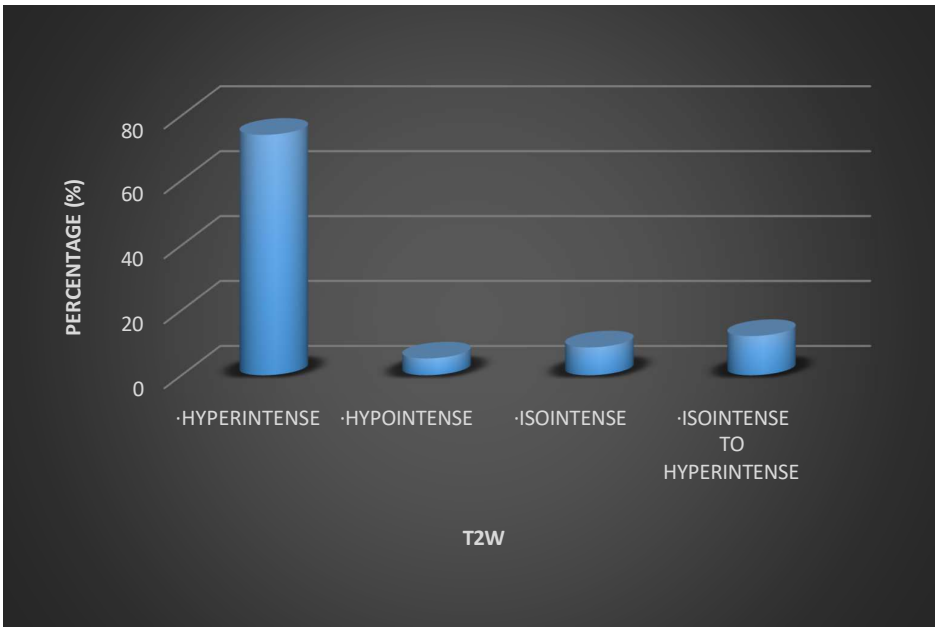

TABLE 10: NECROTIC AREAS- FREQUENCY DISTRIBUTION OF SOLID LESIONS STUDIED

NECROTIC AREAS	NO. OF SOLID LESIONS (N=22)	%
Absent	12	54.5
Present	10	45.5

Among the solid lesions studied, 10 (45.5%) had necrotic areas within them, and 12 lesions (54.5%) had absent necrotic regions.

GRAPH 9: NECROTIC AREAS- FREQUENCY DISTRIBUTION OF SOLID LESIONS STUDIED

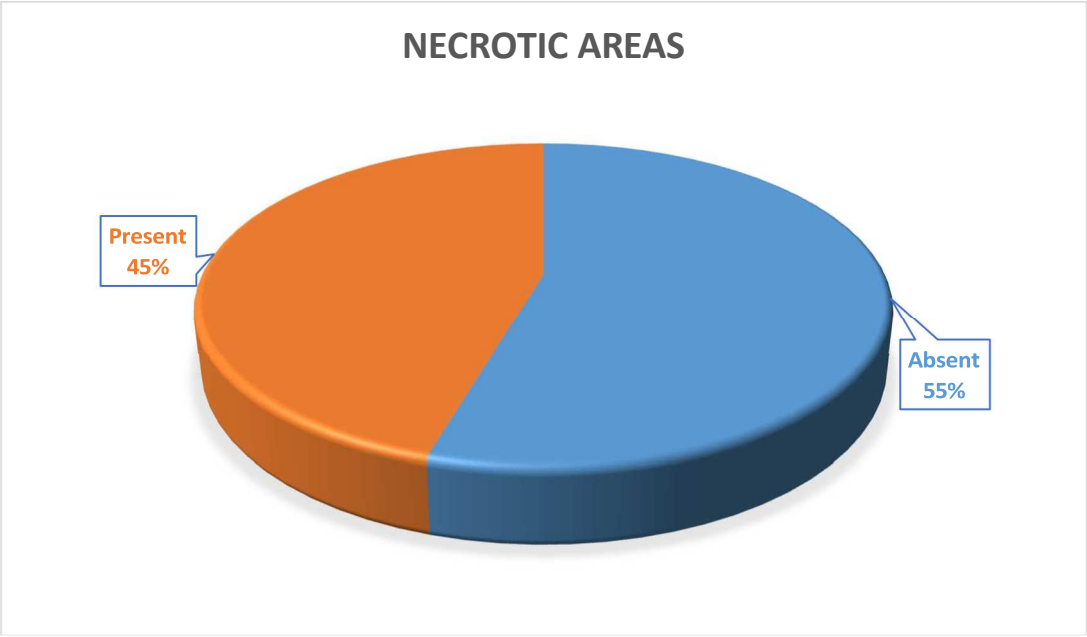

TABLE 11: SEPTATIONS- FREQUENCY DISTRIBUTION OF CYSTIC & COMPLEX CYSTIC LESIONS STUDIED

SEPTATIONS	NO. OF LESIONS (n=36)	%
ABSENT	28	77.3
PRESENT	8	22.7
• FEW THIN SEPTATIONS	5	13.8
• MULTIPLE THICK SEPTATIONS	1	2.7
• ONE THICK SEPTATION	1	2.7
• THICK IRREGULAR SEPTATION	1	2.7

Among the 36 cystic and complex cystic lesions studied, septations were absent in 77.3% and present in 22.7%.

GRAPH 10.1: TYPE OF SEPTATIONS- FREQUENCY DISTRIBUTION OF CYSTIC LESIONS STUDIED

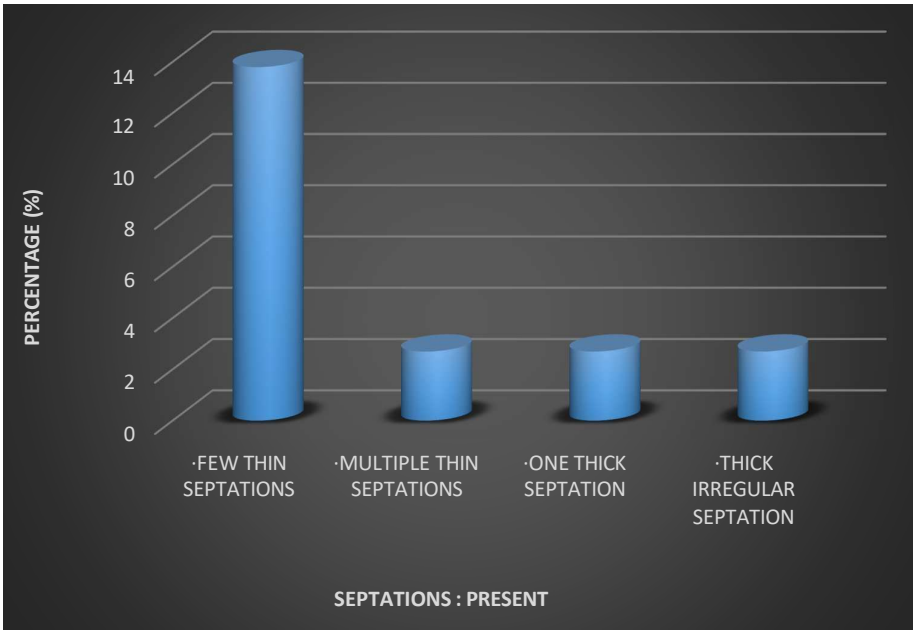

GRAPH 10.2: SEPTATIONS- FREQUENCY DISTRIBUTION OF CYSTIC LESIONS STUDIED

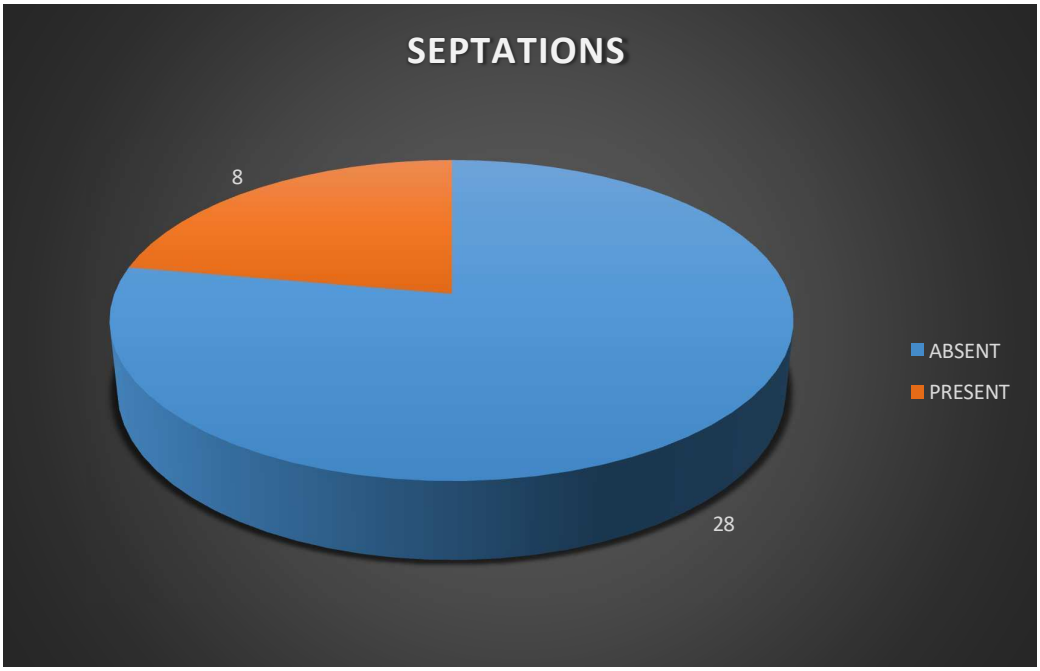

TABLE 12: DIFFUSION RESTRICTION- FREQUENCY DISTRIBUTION OF LESION STUDIED

DIFFUSION RESTRICTION	No. of Lesions (n=58)	%
Absent	33	56.9
Present	25	43.1

Among the 58 lesions studied, 33 had absent restricted diffusion, and 25 had restricted diffusion.

GRAPH 11: DIFFUSION RESTRICTION- FREQUENCY DISTRIBUTION OF LESIONS STUDIED

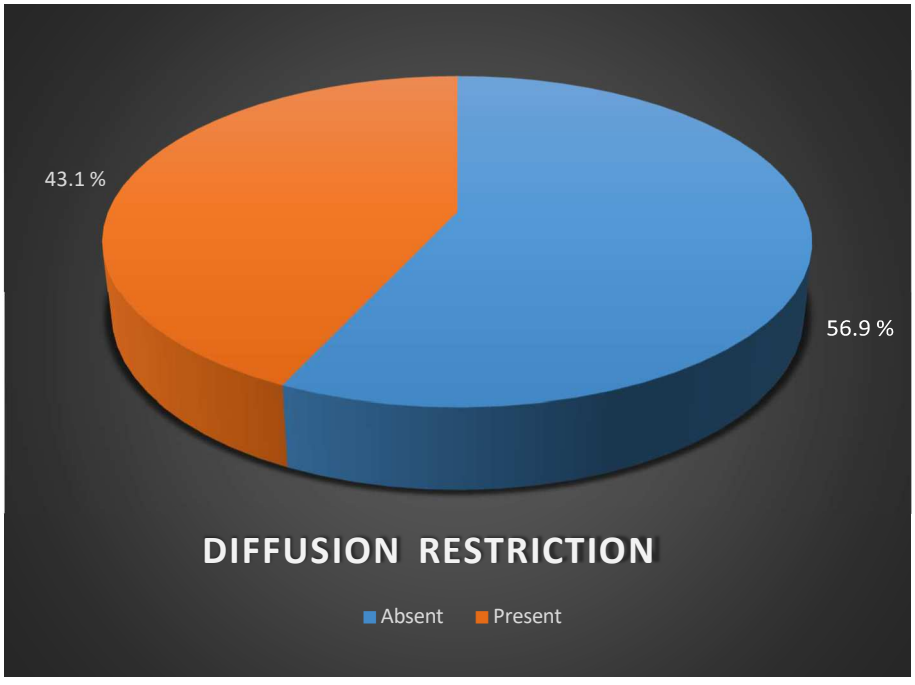

TABLE 13: ADC VALUES (x 10-3 MM2/SEC)- FREQUENCY DISTRIBUTION OF LESIONS STUDIED

ADC VALUES (x 10-3 mm2/sec)	No. of Lesions (n=58)	%
Up to 1.0	7	12.1
1.0-2.0	13	22.4
2.1-3.0	22	37.9
3.1-4.0	16	27.6
Mean	2.36	
S. D	0.99	

Among the lesions studied, 37.9% had ADC values ranging from 2.0 to 3.0, and 27.6% had ADC values ranging from 3.1 to 4.0.

GRAPH 12: ADC VALUES (X 10-3 MM2/SEC)- FREQUENCY DISTRIBUTION OF LESIONS STUDIED

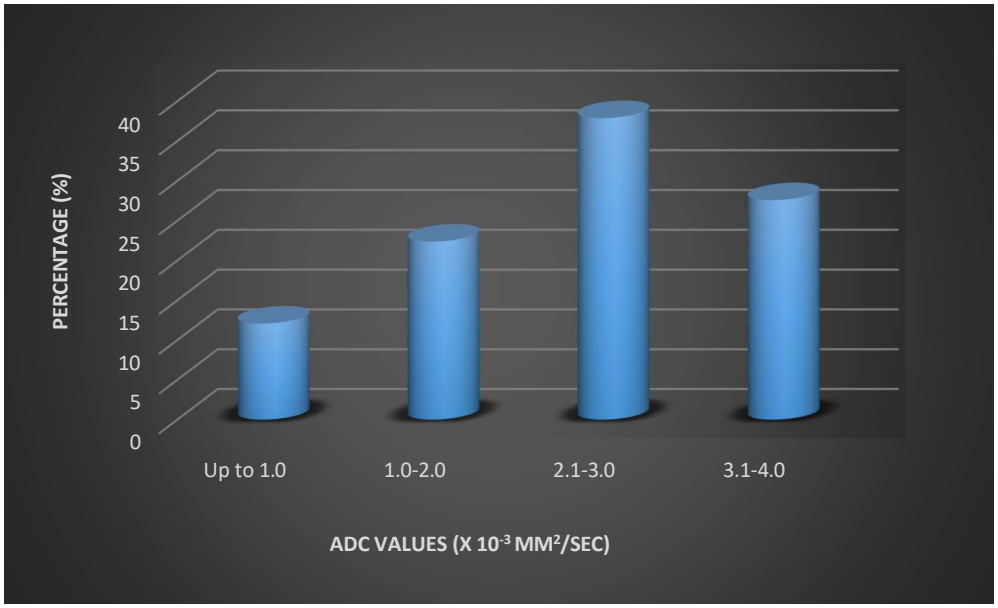

TABLE 14: FINAL DIAGNOSIS- FREQUENCY DISTRIBUTION OF LESIONS STUDIED

Final Diagnosis	**No. of Lesions (n=58)**	**%**
BENIGN	36	63.8
MALIGNANT	22	36.2

Among the lesions studied, 22 lesions suspected of malignancy were taken for histopathological correlation, and biopsy reports were obtained.

GRAPH 13: FINAL DIAGNOSIS- FREQUENCY DISTRIBUTION OF LESIONS STUDIED

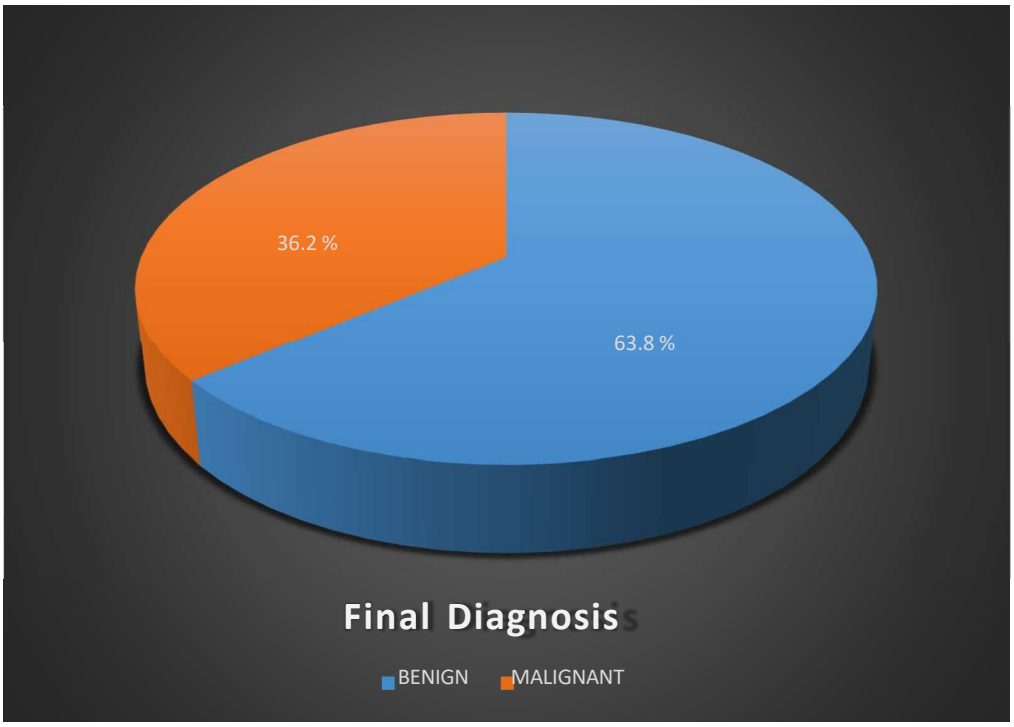

TABLE 15: ASSOCIATION OF MRI IMAGING VARIABLES WITH FINAL DIAGNOSIS OF LESIONS STUDIED,

Variables	FINAL DIAGNOSIS		Total (n=58)	P Values
	BENIGN (n=36)	MALIGNANT (n=22)		
SIZE <4CM	28(77.8%)	6(27.3%)	34(58.6%)	<0.001**
SIZE 4-8 CM	6(16.7%)	9(40.9%)	15(25.9%)	0.082+
SIZE >8 CM	2(5.6%)	7(31.8%)	9(15.5%)	0.011*
SOLID LESION	0(0%)	21(95.5%)	21(36.2%)	<0.001**
CYSTIC LESION	33(91.7%)	1(4.5%)	34(58.6%)	<0.001**
COMPLEX CYSTIC LESION	1(2.8%)	1(4.5%)	2(3.4%)	1.000
T1W				
• HYPERINTENSE	1(2.8%)	2(9.1%)	3(5.2%)	0.550
• HYPOINTENSE	35(97.2%)	11(50%)	46(79.3%)	<0.001**
• HYPOINTENSE TO ISOINTENSE	0(0%)	2(9.1%)	2(3.4%)	0.144
• ISOINTENSE	1(2.8%)	6(27.3%)	7(12.1%)	0.009**
T2W				
• HYPERINTENSE	34(94.4%)	7(31.8%)	41(70.7%)	<0.001**
• HYPOINTENSE	0(0%)	3(13.6%)	3(5.2%)	0.052+
• ISOINTENSE	0(0%)	5(22.7%)	5(8.6%)	0.006**
• ISOINTENSE TO HYPERINTENSE	1(2.8%)	6(27.3%)	7(12.1%)	0.009**

Variables	FINAL DIAGNOSIS		Total (n=58)	P Values
	BENIGN (n=36)	MALIGNANT (n=22)		
NECROTIC AREAS				
• Absent	36(100%)	12(54.5%)	48(82.8%)	<0.001**
• Present	0(0%)	10(45.5%)	10(17.2%)	
SEPTATIONS				
• Absent	28(77.8%)	22(100%)	50(86.2%)	0.019*
• Present	8(22.2%)	0(0%)	8(13.8%)	
• FEW THIN SEPTATIONS	5(13.9%)	0(0%)	5(8.6%)	
• MULTIPLE THIN SEPTATIONS	1(2.8%)	0(0%)	1(1.7%)	
• ONE THICK SEPTATION	1(2.8%)	0(0%)	1(1.7%)	
• THICK IRREGULAR SEPTATION	1(2.8%)	0(0%)	1(1.7%)	
DIFFUSION RESTRICTION				
• Absent	32(88.9%)	1(4.5%)	33(56.9%)	<0.001**
• Present	4(11.1%)	21(95.5%)	25(43.1%)	

Chi-Square Test/Fisher Exact Test

GRAPHS 14.1: ASSOCIATION OF SIZE WITH FINAL DIAGNOSIS OF LESIONS STUDIED,

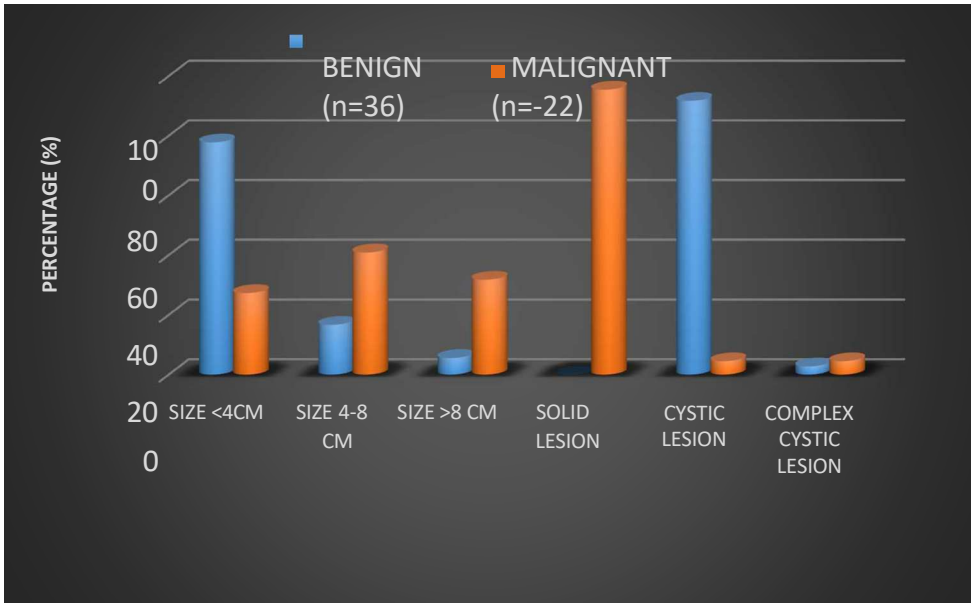

GRAPHS 14.2: ASSOCIATION OF T1 SIGNAL INTENSITY WITH FINAL DIAGNOSIS OF LESIONS STUDIED,

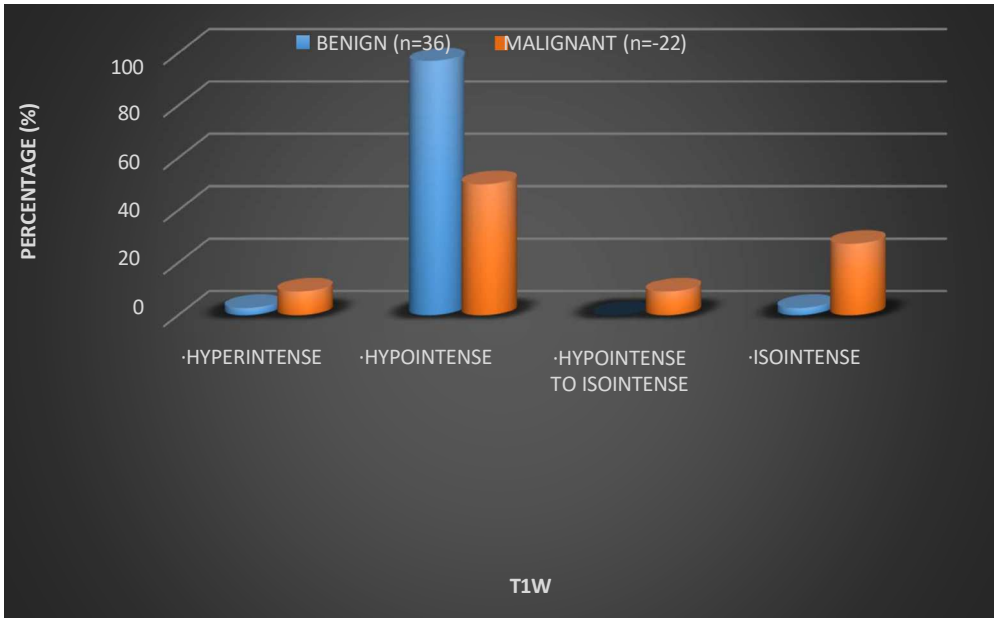

GRAPHS 14.3: ASSOCIATION OF T2 SIGNAL INTENSITY WITH FINAL DIAGNOSIS OF LESIONS STUDIED,

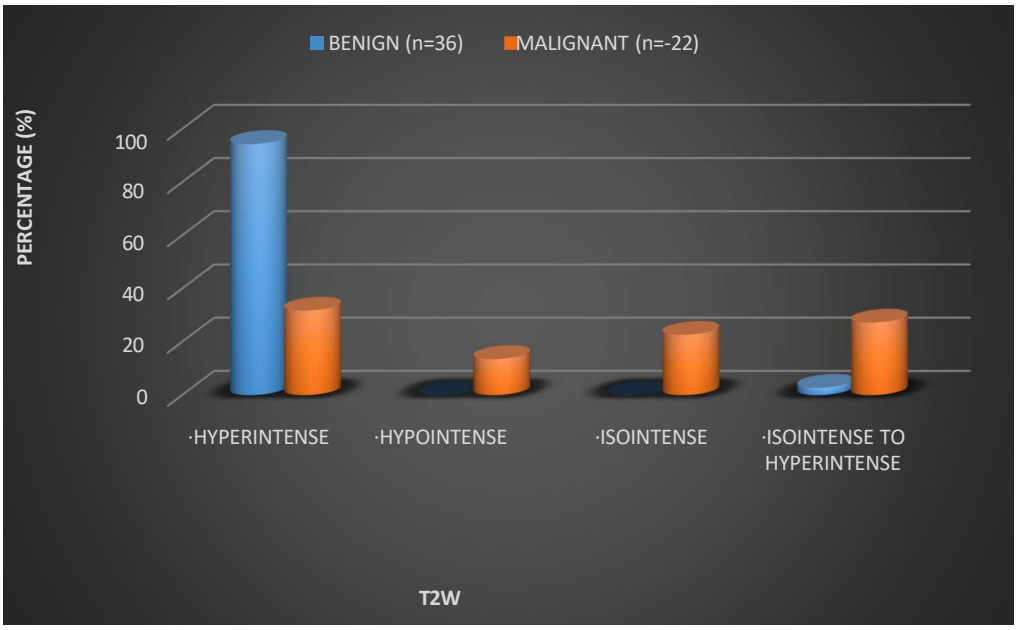

GRAPHS 14.4: ASSOCIATION OF NECROTIC AREAS WITH FINAL DIAGNOSIS OF LESIONS STUDIED,

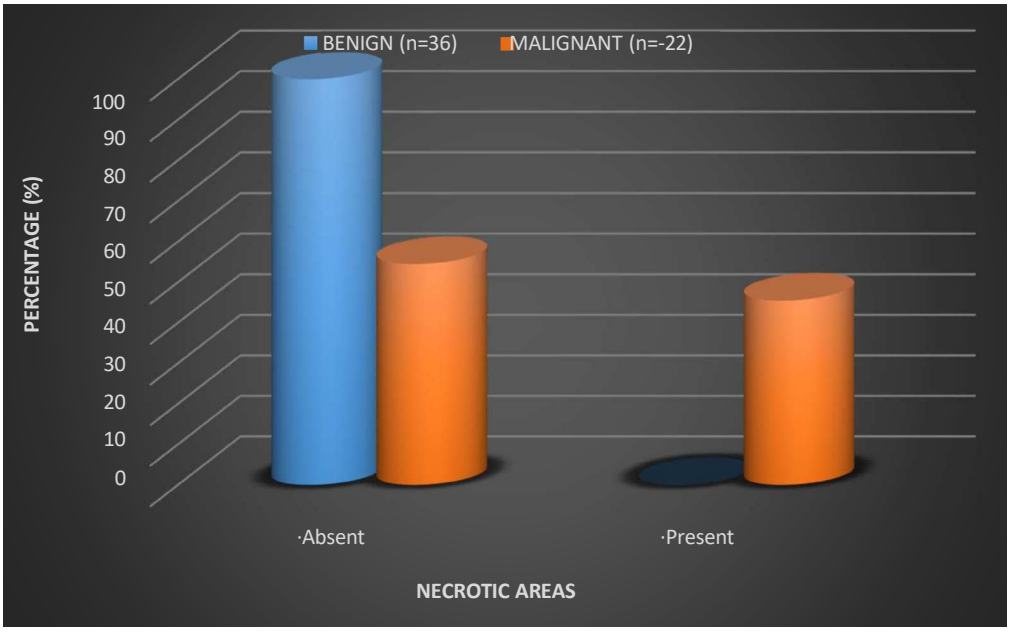

GRAPHS 14.5: ASSOCIATION OF SEPTATIONS WITH FINAL DIAGNOSIS OF LESIONS STUDIED,

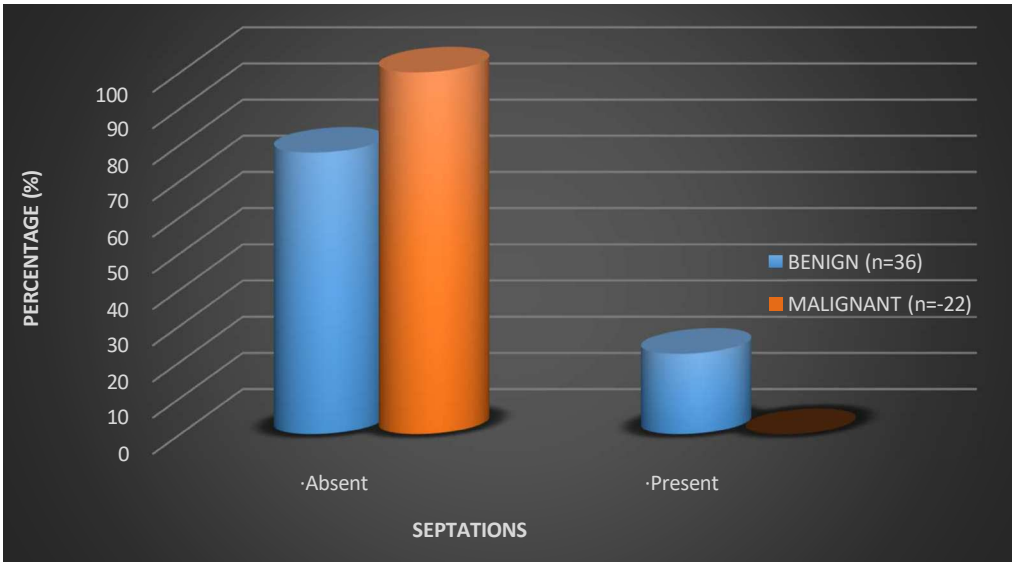

GRAPHS 14.6: ASSOCIATION OF TYPE OF SEPTATIONS WITH FINAL DIAGNOSIS OF LESIONS STUDIED,

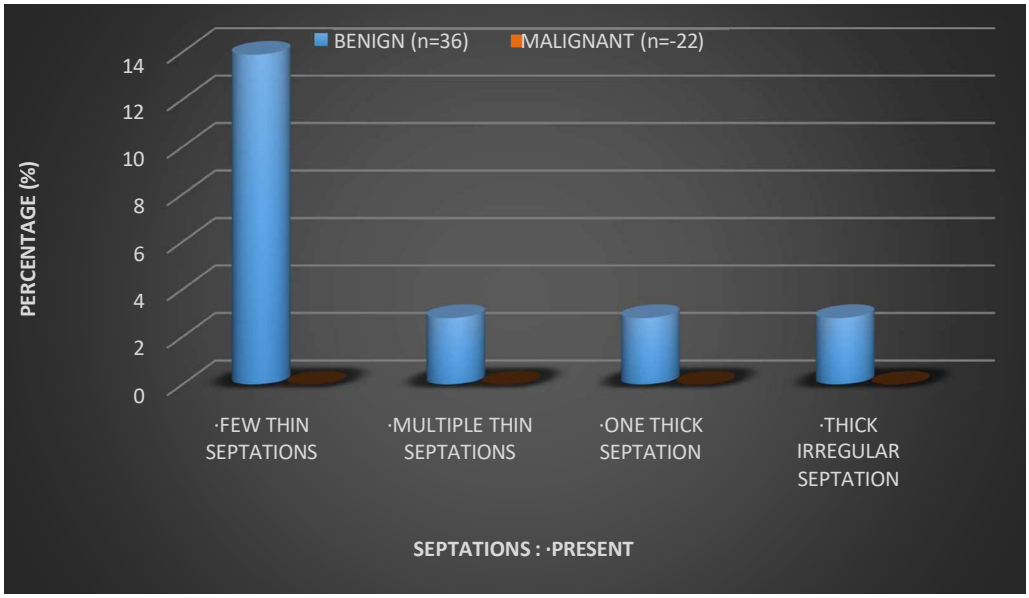

GRAPHS 14.7: ASSOCIATION OF DIFFUSION RESTRICTION WITH FINAL DIAGNOSIS OF LESIONS STUDIED,

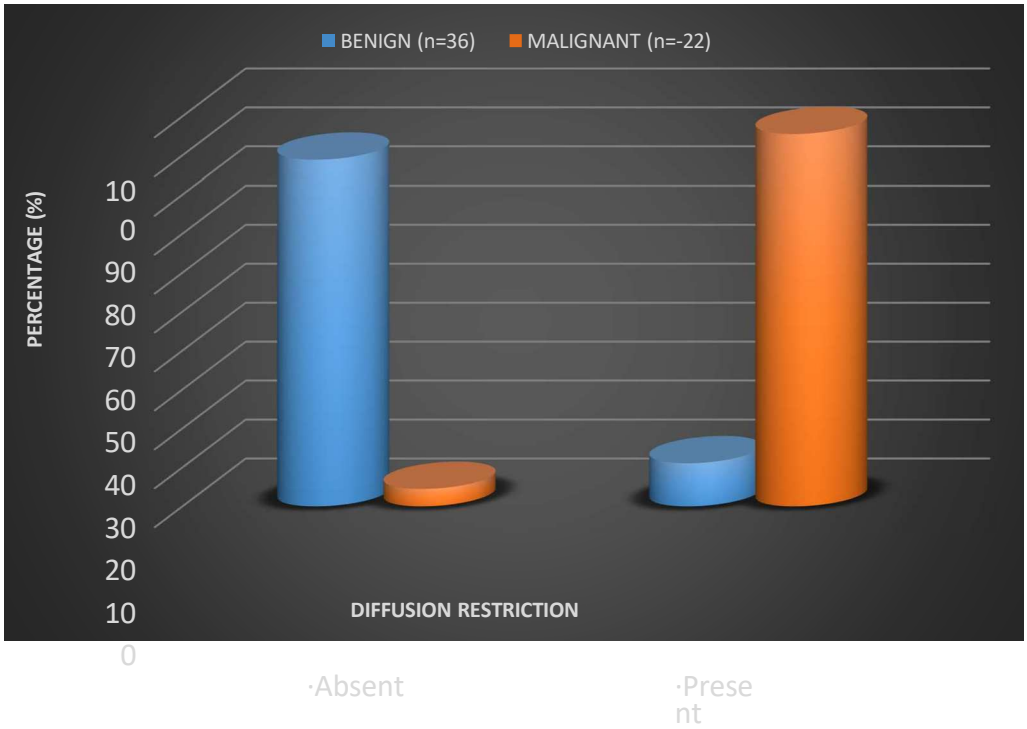

TABLE 16: ADC VALUES (X 10^{-3} MM^2/SEC)- ABOUT THE FINAL DIAGNOSIS OF PATIENTS STUDIED

ADC VALUES (x 10^{-3} mm^2/sec)	FINAL DIAGNOSIS		Total (n=58)
	BENIGN (n=36)	MALIGNANT (n=22)	
Up to 1.0	0(0%)	6(27.3%)	6(12.1%)
1.0-2.0	2(5.6%)	12(54.5%)	14(22.4%)
2.1-3.0	18(50%)	4(18.2%)	22(37.9%)
3.1-4.0	16(44.4%)	0(0%)	16(27.6%)
Mean ± SD	3±0.6	1.32±0.53	2.36±1

P≤0.001**, Significant, Student t Test

Among the benign and cystic lesions studied, 50% of benign lesions had ADC values between 2.0 and 3.0, while 44.4% of lesions had ADC values between 3.0 and 4.0. 54.5 % of malignant lesions had ADC values between 1.0 and 2.0, while 27.3% had ADC values less than 1.0.

GRAPH 15: ADC VALUES (X 10^{-3} MM^2/SEC)- ABOUT THE FINAL DIAGNOSIS OF PATIENTS STUDIED

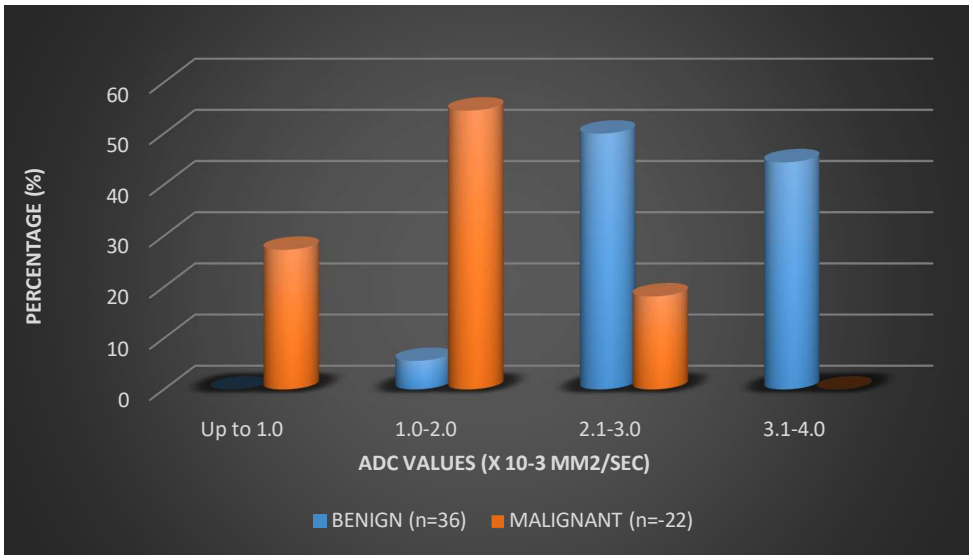

TABLE 17: ADC VALUES (X 10^{-3} MM^2/SEC)- IN RELATION TO CLEAR CELL RCC & NON-CLEAR CELL RCC OF PATIENTS STUDIED:

ADC VALUES (x 10-3 mm2/sec)	**CLEAR CELL RCC & OTHER RCC**		**Total (n=22)**
	CLEAR CELL RCC (n=11)	**OTHER CELL RCC (n=11)**	
Up to 1.0	0(0%)	6(60.0%)	6(23.8%)
1.0-2.0	7(63.6%)	5(40.0%)	12(52.4%)
2.1-3.0	4(36.4%)	0(0%)	4(19%)
3.1-4.0	0(0%)	0(0%)	0(0%)
Mean ± SD	1.73±0.42	0.90±0.29	1.32±0.35

P≤0.001**, Significant, Student t Test

Among 22 malignant lesions studies, clear cell RCC had a mean ADC value of 1.73 ± 0.42, while non-clear cell carcinomas had mean ACDC values of 0.90 ± 0.29.

GRAPH 16.1: RANGE OF ADC VALUES (X 10^{-3} MM^2/SEC)- IN RELATION TO CLEAR CELL RCC & NON-CLEAR CELL RCC OF PATIENTS STUDIED:

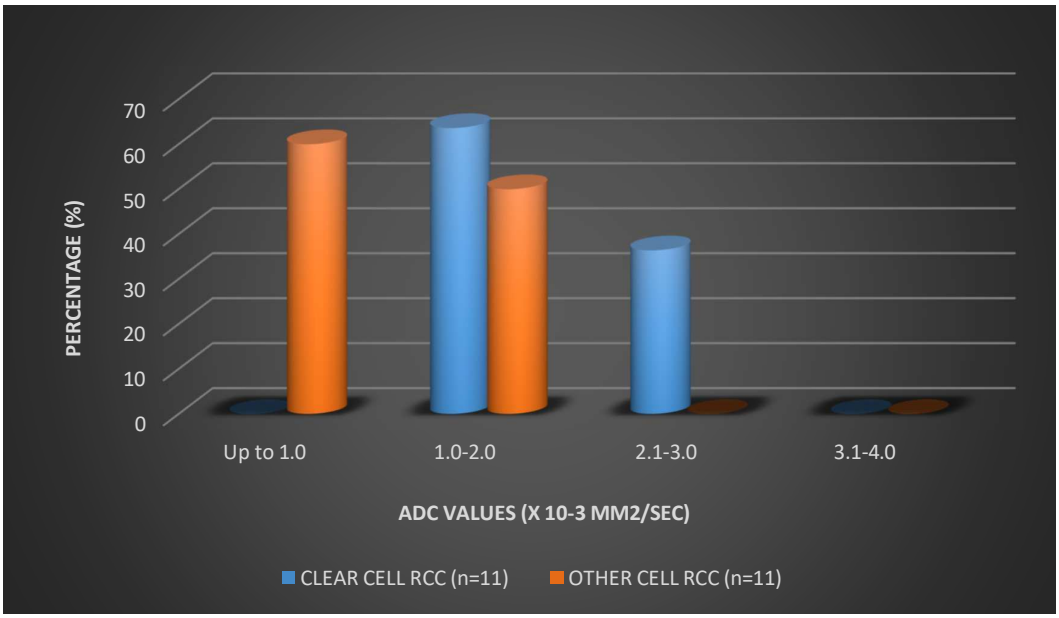

GRAPH 16.2: BOX AND WHISKER PLOT FOR A RANGE OF ADC VALUES (X 10^{-3} MM^2/SEC)- ABOUT CLEAR CELL RCC & NON-CLEAR CELL RCC OF PATIENTS STUDIED:

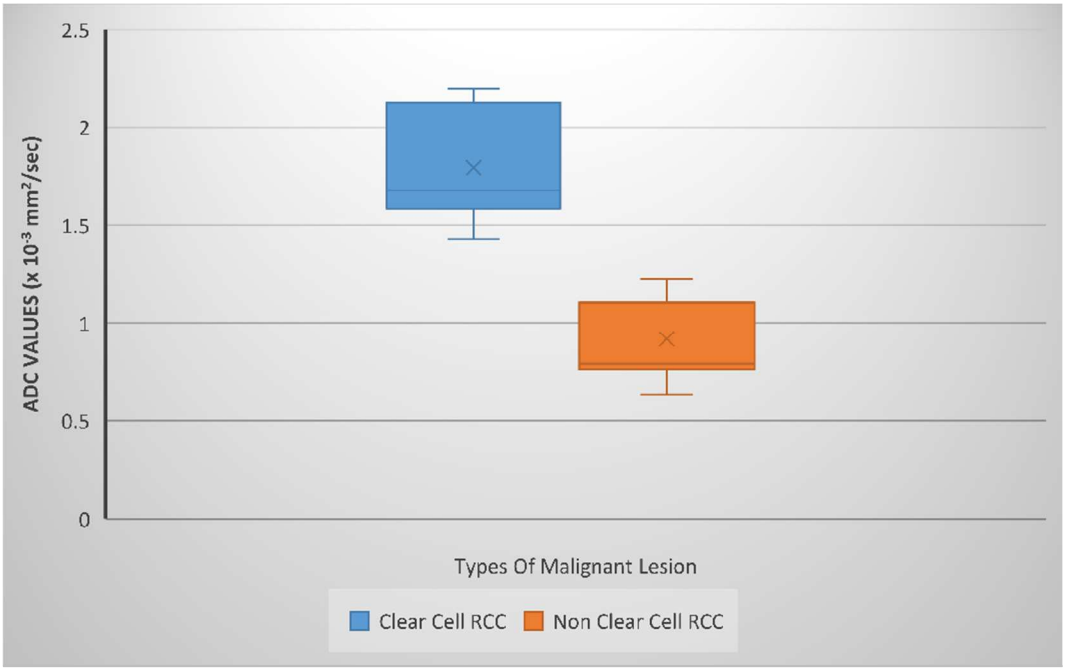

TABLE 18: ADC VALUES (X 10^{-3} MM^2/SEC)- ABOUT THE TYPE OF CYSTIC LESIONS STUDIED,

ADC VALUES (x 10^{-3} mm^2/sec)		**TYPE OF CYSTIC LESION**				**Total (n=36)**
	Bosniak type I cyst	**Bosniak type II cyst**	**Bosniak type IIF cyst**	**Bosniak type III cyst**	**Bosniak type IV cyst**	
Up to 1.0	0(0%)	0(0%)	0(0%)	0(0%)	0(0%)	0(0%)
1.0-2.0	0(0%)	0(0%)	0(0%)	0(0%)	0(0%)	0(0%)
2.1-3.0	8(32.0%)	4(50%)	0(0%)	1(50%)	1(100%)	13(37%)
3.1-4.0	17(68.0%)	4(50%)	0(0%)	1(50%)	0(0%)	21(45.7%)
Total	25(100%)	8(100%)	0(0%)	2(100%)	1(100%)	36(100%)
Mean ± SD	3.06±0.64	2.97±0.12		3.22±0.33	2.11±0	2.72±0.078

F=12.497; p<0.001**; ANOVA TEST

Reference: Silverman SG, Pedrosa I, Ellis JH, Hindman NM, Schieda N, Smith AD, et al. Bosniak classification of cystic renal masses, version 2019: An updated proposal and needs assessment. Radiology. 2019;292(2):475–88. Available from: http://dx.doi.org/10.1148/radiol.2019182646

GRAPH 17.1: ADC VALUES (X 10^{-3} MM^2/SEC)- ABOUT THE TYPE OF CYSTIC LESIONS STUDIED,

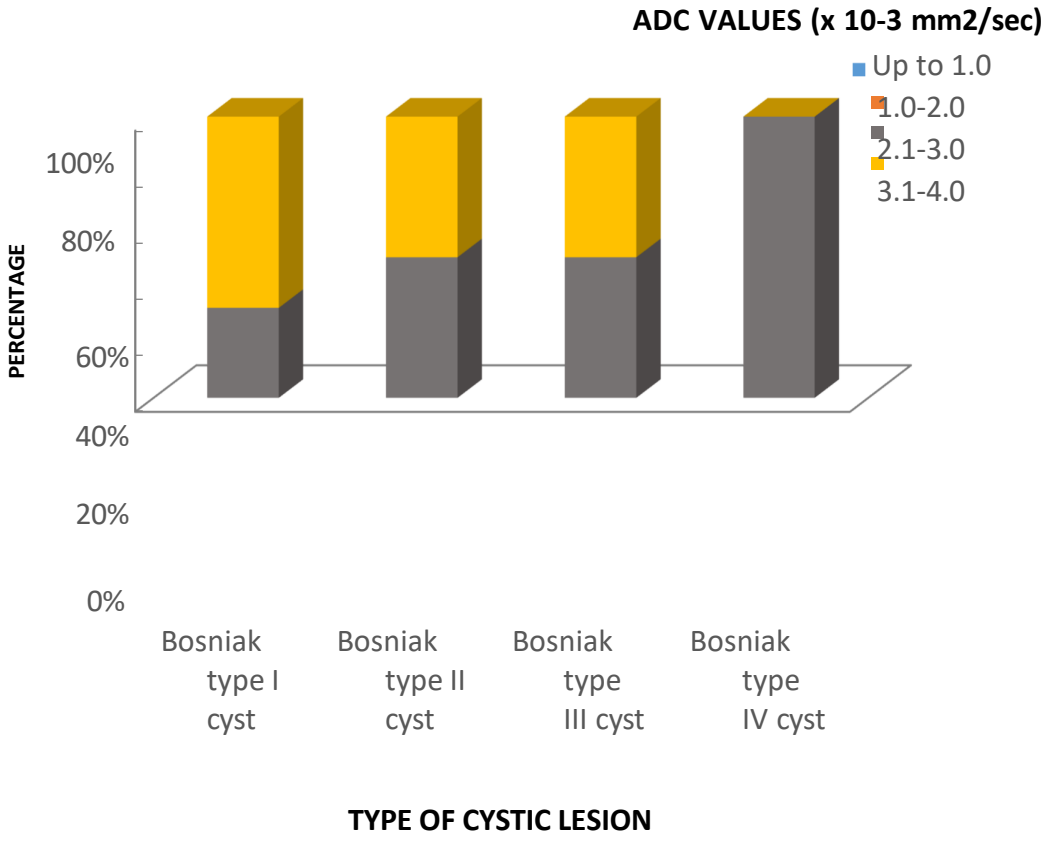

GRAPH 17.2: BOX AND WHISKER PLOT FOR A RANGE OF ADC VALUES (X 10^{-3} MM^2/SEC)- ABOUT THE TYPE OF CYSTIC LESIONS STUDIED,

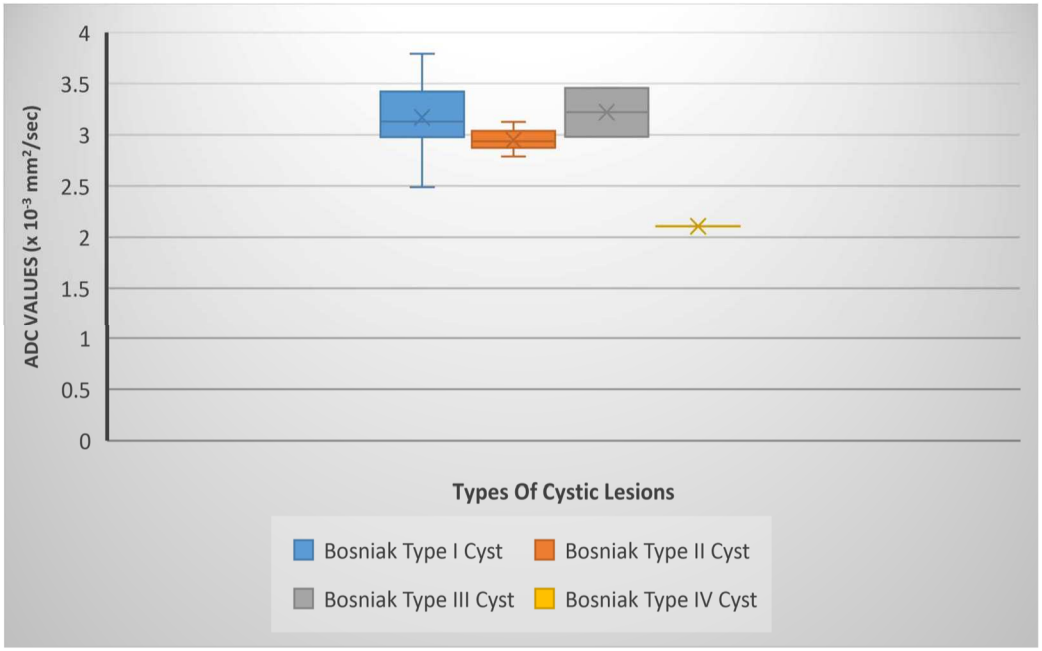

TABLE 19: ADC VALUES (X 10^{-3} MM^2/SEC)- ABOUT THE TYPE OF MALIGNANT LESIONS STUDIED

ADC VALUES (x 10-3 mm2/sec)	**TYPE OF MALIGNANT LESION**					**Total**
	Clear cell RCC	**Chromophobe type RCC**	**Papillary type RCC**	**Transitional cell carcinoma**	**Wilms tumor**	
Up to 1.0	0(0%)	1(33.3%)	0(0%)	0(0%)	5(100%)	6(28.6%)
1.0-2.0	7(63.6%)	2(66.7%)	2(100%)	1(100%)	0(0%)	11(52.4%)
2.1-3.0	4(36.4%)	0(0%)	0(0%)	0(0%)	0(0%)	4(19%)
3.1-4.0	0(0%)	0(0%)	0(0%)	0(0%)	0(0%)	0(0%)
Total	11(100%)	3(100%)	2(100%)	1(100%)	5(100%)	22(100%)
Mean ± SD	1.73±0.42	0.83±0.04	1.15±0.19	1.23±0.10	0.76±0.14	1.14±0.24

F=8.326; p=0.001**; ANOVA TEST

GRAPH 18.1: ADC VALUES (X 10-3 MM2/SEC)- ABOUT MALIGNANT LESIONS OF PATIENTS STUDIED,

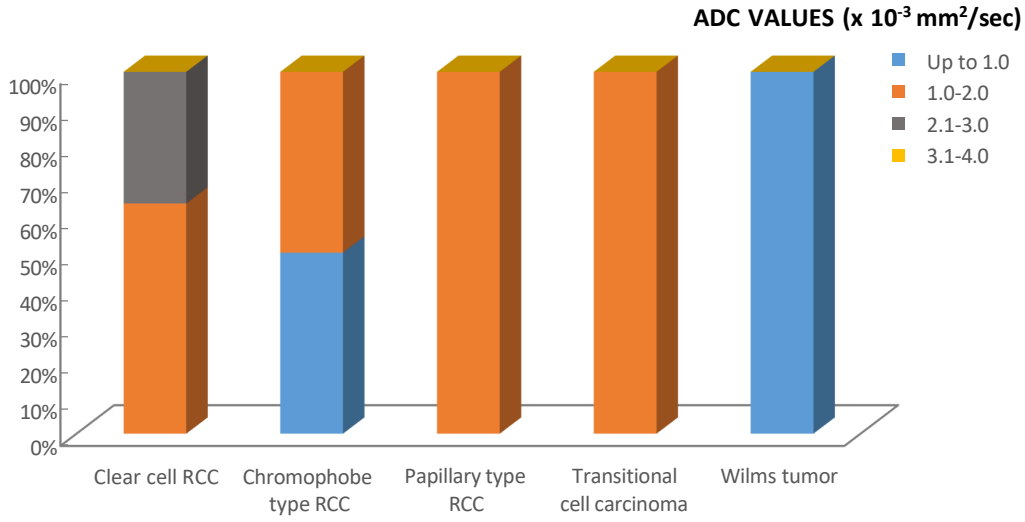

GRAPH 18.2: BOX AND WHISKER PLOT FOR A RANGE OF ADC VALUES (X 10^{-3} MM^2/SEC)- ABOUT MALIGNANT LESIONS OF PATIENTS STUDIED

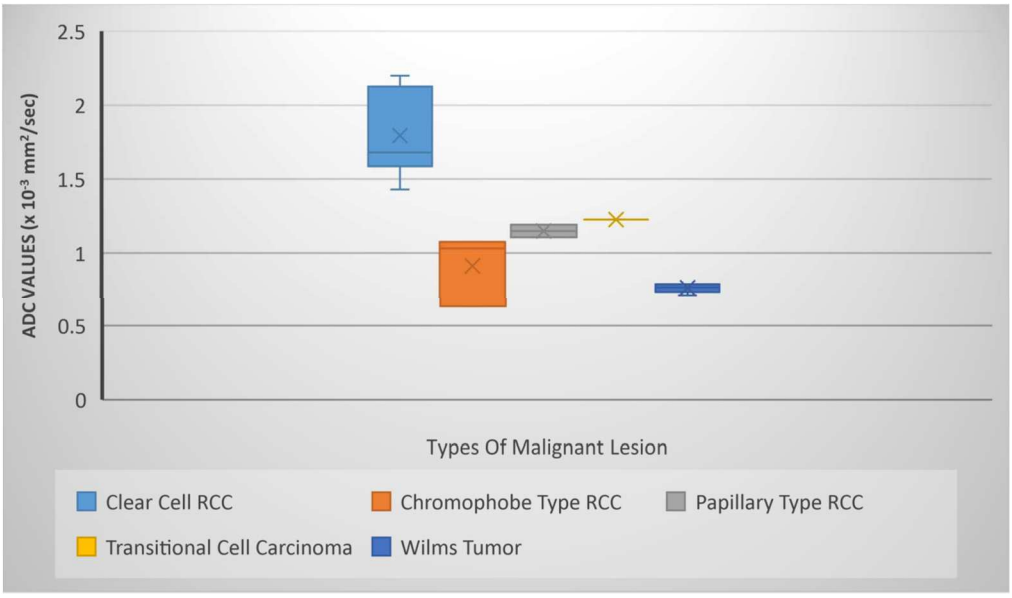

DISCUSSION

This research is significant as it unveils novel findings on the diagnostic utility of apparent diffusion coefficient (ADC) and diffusion-weighted imaging (DWI) in differentiating between renal masses. The potential impact on therapy choices and patient care makes this a crucial area of investigation. The study's unique contribution lies in its potential to enhance renal parenchymal disease, infection, and tumour diagnosis through comprehensive ADC measurement. [5, 10, 11, 13, 35]

The research underscores the practical implications of diffusion-weighted MR imaging in diagnosing diffuse parenchymal abnormalities and focal lesions in abdominal organs. The study by Yamamoto et al. [54] is particularly noteworthy, as it revealed that malignant masses' apparent diffusion coefficients (ADCs) were significantly lower than those of benign masses such as hemangiomas and cysts in the liver despite a slight overlap. This underscores the potential of diffusion-weighted imaging in achieving high sensitivity and specificity in distinguishing between malignant and benign liver lesions. [57,58]

It has been discovered that ADCs and renal function are correlated with one another [16,28,62]. A few recent investigations have demonstrated the feasibility and reliability of diffusion-weighted imaging in evaluating renal function [10,60]. However, more research is needed to assess focal renal masses. Few studies have examined the use of diffusion-weighted imaging for assessing localised renal lesions, despite the inclusion of renal lesions occasionally in studies examining the methodology, efficacy, and usefulness of DWI in abdominal imaging in general [56,61,64]. This highlights the need for further research in this area.

The majority of the participants in the study belonged to the age group of 50- 60 years (34.1%), followed by 60-70 years (20.5%). The least number of participants in the study belonged to the age group of 10-20 and 20-30 years [each 2.3% respectively].

In the present study, males outnumbered females (61.4% males & 38.6% females). About one-fourth of the patients presented with no symptoms. The remaining three-fourths of the patients (n=33) presented with varied symptoms like abdominal pain, abdominal distension, hematuria, weight loss, etc. The most common presenting symptoms were abdominal pain (61.4%) and hematuria (29.5%). The least common symptoms were nausea and vomiting (each 2.3%, respectively). Symptoms were observed primarily in patients with malignant rather than benign lesions.

The study included 44 patients, with 58 lesions observed. These lesions were categorised into 36 cystic lesions (58.6%), 22 solid lesions (36.2%), and two complex-cystic lesions (3.4%). Solid lesions underwent histopathological correlation, while cystic lesions were either not intervened or followed up with imaging.

Most benign cystic lesions (77.8%) are less than 4.0 cm in size, whereas most malignant lesions (72.7%) are usually larger than 4.0 cm.

T1 hypointense and T2 hyperintense changes are the most common imaging findings among benign and malignant lesions. They are more commonly seen with benign cystic lesions (94.4% and 94.6% of cases, respectively) than with their malignant counterparts, which denotes the cystic fluid nature of the lesion.

While T2 hyperintense signal is the most common imaging finding with malignant lesions (seen in 31.8% of cases), it usually correlates with the necrotic areas within the lesion (45.5% of cases).

Out of 58 lesions under evaluation, restricted diffusion is absent in 33,

with the most benign (88.9%). Restricted diffusion and low ADC values denote increased cellularity within the lesion, which is seen with 25 lesions. 95.5% of the malignant lesions in our study showed evidence of restricted diffusion. 11.1 % of the benign cysts also showed evidence of restricted diffusion, which may indicate hemorrhagic content within the lesion.

In the 22 patients who had surgical histopathology reports, the tumours were diagnosed as clear cell renal cell carcinoma (n = 11), papillary RCC (n = 2), chromophobe RCC (n =3), transitional cell cancer (n = 1), and Wilms tumour (n = 5). All clear cell RCCs were diagnosed as solid masses on gross pathology. The minimum ADC values used for statistical analysis were usually obtained from the more solid parts of these tumours.

We observed discrepancies in the ADC values between the findings of our investigation and those of Sandrasegaran et al. [6]. Our data fell into a broader range, from 0.79 to 3.6 × 10^{-3} mm^2/s, whereas Sandrasegaran and colleagues reported a range from 1.4 to almost 3.2 × 10^{-3} mm^2/s. These differences are explained by variances in the equipment utilised, which might result in discrepancies in the ADC results. ADC readings can be affected by minute blood flow and magnetic field defects, even though the actual diffusion process remains constant regardless of the magnetic field's intensity. As a result, ADC values tend to be significantly lower, by roughly 2–10%, when measured at higher magnetic field strengths like 3T compared to 1.5 T [65,66].

Determining ADC values also depends on the choice of b values. Lower ADC readings are usually the result of higher b values (more than 500 s/mm^2), which are more accurate in recording actual diffusion [68]. Furthermore, Sandrasegaran and colleagues employed minimum ADC values, similar to our work, which

concentrated on the minimum of the mean ADC measurements.

Focusing on minimum ADC measurements makes us more likely to capture the most densely cellular areas within tumours. Studies on brain tumours support this approach [67,65,68,66]. Because we used minimum ADC measurements, we didn't need to distinguish between entirely solid tumours and those with some necrotic (dead tissue) areas. Our measurements were explicitly taken from the solid parts of the tumour, simplifying the process.

Few findings of our investigation are consistent with those of Sandrasegaran et al., demonstrating that benign cystic lesions typically have greater ADCs ($2.72 \pm 0.78 \times 10^{-3}$ mm²/s) than malignant ones ($1.32 \pm 0.5 \times 10^{-3}$ mm²/s). Studies on liver lesions have also reported this association [56, 58]. Furthermore, we discovered that complex benign cysts show less diffusion than simple cysts when they contain more blood or protein [5]. Diffusion may be reduced in complicated cysts due to more giant molecules or cellular debris obstructing the diffusion process.

Numerous discussions have been held in the neurological literature on the application of DWI in assessing tumour grade. Most non-clear cell renal cell carcinomas (RCCs) in our study were of the papillary or chromophobe histologic subtypes, which often have a better prognosis than clear cell RCCs. ADCs of non-clear cell RCCs were shown to tend to be lesser ($0.90 \pm 0.3 \times 10^{-3}$ mm²/s) than those of clear cell RCCs. On the other hand, only clear cell RCCs showed an ADC value of less than $1.73 \pm 0.42 \times 10^{-3}$ mm²/s.

The study's findings are noteworthy, implying that renal lesions with different tissue compositions have variable diffusion properties. The potential of diffusion-weighted imaging (DWI) in characterising renal lesions is highlighted by the decreased apparent diffusion coefficients (ADCs) reported in solid tumour tissue

relative to necrotic or cystic tumour tissue, with even lower ADCs in benign cysts.

The link between the properties of the ADC and T1 signals further complicates lesion distinction. It seems sensible to speculate that blood or proteinaceous materials may affect the strength of the T1 signal; this has been observed in other situations, such as brain haemorrhage [69,70]. Hemorrhagic products dynamically evolve in the brain over time, which may be similar to how chronic haemorrhage affects ADC values for renal lesions.

This is because the hemorrhagic product in the brain experiences a progressive change in chemical composition over time. If a kidney lesion is present, there's a chance that the bleeding is primarily chronic at the imaging time, which might mean that it only affects ADC values in one direction. Benign cysts may be distinguished from necrotic or cystic tumours with a bit of overlap in ADCs when both ADC values and T1 characteristics are considered.

CONCLUSION

1. DWI MRI of the kidney appears to be a viable and accurate approach for distinguishing between normal renal parenchyma and various renal disorders.
2. DWI is most helpful for patients for whom gadolinium is contraindicated.
3. It gives quantitative data regarding diffusivity together with diagnostic-quality DWI pictures.
4. DWI can differentiate cystic benign lesions from cystic renal cell carcinoma, making it a valuable tool in evaluating renal masses.
5. DWI aids in the differentiation of various subgroups of renal cell carcinoma and helps in categorising renal cell carcinomas compared to other non-renal cell carcinomas.
6. ADC maps with b values of 0 and 800 s/mm2 can be used as an imaging biomarker in the histological subtyping of renal cell carcinoma.
7. The ADC of a kidney lesion appears to correlate with its T1 signal.

SUMMARY

- This study was a one-year hospital-based observational study.
- 44 patients were included in the study by the inclusion and exclusion criteria.
- DWI sequence was included in all these MRI abdomen studies along with conventional MR sequences.
- The study aimed to understand the use and applications of DWI in evaluating renal masses using ADC values and to narrow the differential diagnosis, which helps to interpret the final diagnosis.
- Diffusion-weighted imaging is based on the movement of water molecules and provides information about tissue architecture and integrity. It assists early metastasis detection, evaluates therapy response, and distinguishes benign from malignant tumours in cancer imaging.
- 58 lesions were included in the study, of which 22 lesions proved malignant by histopathological evaluation, while the rest were benign cystic lesions.
- Benign cystic lesions were categorised by the Bosniak classification system 2019.
- Benign cystic lesions of various categories have higher ADC values with a mean of $2.72 \pm 0.78 \times 10^{-3}$ mm²/s (Mean ± SD).
- Malignant lesions are clear cell RCC, chromophobe type RCC, papillary type RCC, transitional cell carcinoma, and Wilms tumour.
- Malignant lesions had varied ADC values, with clear cell renal cell carcinoma (ccRCC) having ADC values ($1.73 \pm 0.42 \times 10^{-3}$ mm²/s) higher than non-clear cell renal cell carcinoma ($0.90 \pm 0.29 \times 10^{-3}$ mm²/s), which helps in diagnosis and treatment.
- Lowest ADC values are noted with Wilms tumour with a mean of $0.76 \pm 0.14 \times 10^{-3}$ mm²/s

LIMITATIONS

Acknowledging the limitations of our study is essential for understanding the scope and potential implications of our findings.

1. Our analysis was limited to individuals with histopathologically verified results, leading to a small patient sample. This calls for further studies with larger patient populations and a broader range of tumour types. Confirming our preliminary findings in a more diverse cohort would strengthen the validity and applicability of our conclusions, potentially leading to advancements in the characterisation and management of renal lesions.
2. In unstable patients and patients with claustrophobia, the quality of the images was poor.
3. An MRI of the abdomen is an expensive investigation compared to CT.
4. A contrast study was not done along with DWI, which would have further improved the characterisation of the lesion.
5. A prolonged period of stability on imaging tests could not confirm the diagnosis of a benign lesion.

BIBLIOGRAPHY

1. Maria Assunta Cova, Ettore Squillaci, Fulvio Stacul, Guglielmo Manenti, Gava S, Simonetti G, et al. Diffusion-weighted MRI in the evaluation of renal lesions: preliminary results. British Journal of Radiology. 2004 Oct 1;77(922):851–7.
2. Bosniak MA. The current radiological approach to renal cysts. Radiology 1986 Jan 1;158(1):1–10.
3. Silverman SG, Pedrosa I, Ellis JH, Hindman NM, Schieda N, Smith AD, et al. Bosniak Classification of Cystic Renal Masses, Version 2019: An Update Proposal and Needs Assessment. Radiology. 2019 Aug;292(2):475–88.
4. Mirka H, Korcakova E, Kastner J, Hora M, Hes O, Hosek P, et al. Diffusion-weighted Imaging Using 3.0 T MRI as a Possible Biomarker of Renal Tumors. Anticancer Research. 2015 Apr 1;35(4):2351–7.
5. Zhang J, Yousef Mazaheri Tehrani, Wang L, Ishill N, Schwartz L, Hedvig Hricak. Renal Masses: Characterization with Diffusion-weighted MR Imaging—A Preliminary Experience. Radiology. 2008 May 1;247(2):458–64.
6. Kumaresan Sandrasegaran, Sundaram CP, Ramaswamy R, Fatih Akisik, Rydberg MP, Lin C, et al. The usefulness of Diffusion-Weighted Imaging in the Evaluation of Renal Masses. American Journal of Roentgenology. 2010 Feb 1;194(2):438–45.
7. Suresh de Silva, Lockhart K, Aslan P, Nash PA, Hutton A, Malouf D, et al. The diagnostic utility of diffusion-weighted MRI imaging and ADC ratio to distinguish benign from malignant renal masses: sorting the kittens from the tigers. BMC Urology. 2021 Apr 22;21(1).

8. Bachir Taouli, Thakur R, Di L, Babb JS, Soo Rin Kim, Hecht EM, et al. Renal Lesions: Characterization with Diffusion-weighted Imaging versus Contrast-enhanced MR Imaging. 2009 May 1;251(2):398–407.
9. Israel GM, Hindman N, Bosniak MA. Evaluation of Cystic Renal Masses: Comparison of CT and MR Imaging by Using the Bosniak Classification System. Radiology. 2004 May;231(2):365–71.
10. Carbone SF, Gaggioli E, Ricci V, Mazzei F, Mazzei MA, Volterrani L. Diffusion-weighted magnetic resonance imaging in the evaluation of renal function: A preliminary study. La radiologia medica. 2007 Dec;112(8):1201–10.
11. Thoeny HC, Frederik De Keyzer, Oyen R, Peeters R. Diffusion-weighted MR Imaging of Kidneys in Healthy Volunteers and Patients with Parenchymal Diseases: Initial Experience. 2005 Jun 1;235(3):911–7.
12. Nicolau C, Antunes N, Paño B, Sebastia C. Imaging Characterization of Renal Masses. Medicina. 2021 Jan 8;57(1):51.
13. Squillaci E, Manenti G, Cova M, Di Roma M, Miano R, Palmieri G, et al. Correlation of diffusion-weighted MR imaging with cellularity of renal tumours. Anticancer Research. 2004 [cited 2024 Jun 3];24(6):4175–9.
14. Sasaki M, Yamada K, Watanabe Y, Matsui M, Ida M, Fujiwara S, et al. Variability in Absolute Apparent Diffusion Coefficient Values across Different Platforms May Be Substantial: A Multivendor, Multi-institutional Comparison Study. Radiology. 2008 Nov 1;249(2):624–30.
15. Tomohiro Namimoto, Yamashita Y, Katsuhiko Mitsuzaki, Nakayama Y, Tang Y, Takahashi M. Measurement of the apparent diffusion coefficient in diffuse renal disease by diffusion-weighted echo-planar MR imaging. Journal of Magnetic Resonance Imaging. 1999 Jun 1;9(6):832–7.

16. Müller MF, Prasad PV, D Bimmler, Kaiser A, Edelman RR. Functional imaging of the kidney by means of measurement of the apparent diffusion coefficient. Radiology. 1994 Dec 1;193(3):711–5.
17. Siegel CL, Aisen AM, Ellis JH, Londy F, Chenevert TL. Feasibility of MR diffusion studies in the kidney. Journal of magnetic resonance imaging: JMRI [Internet]. 1995 [cited 2024 Jun 3];5(5):617–20.
18. Basic principles of diffusion-weighted imaging. European Journal of Radiology. 2003 Mar 1;45(3):169–84.
19. Backens M. [Basic principles and technique of diffusion-weighted imaging and diffusion tensor imaging]. Der Radiologe. 2015 Sep 1;55(9):762–70.
20. Malayeri AA, El Khouli RH, Zaheer A, Jacobs MA, Corona-Villalobos CP, Kamel IR, et al. Principles and Applications of Diffusion-weighted Imaging in Cancer Detection, Staging, and Treatment Follow-up. RadioGraphics. 2011 Oct;31(6):1773–91.
21. Cercignani M, Horsfield MA. The physical basis of diffusion-weighted MRI. Journal of the Neurological Sciences [Internet]. 2001 May 1 [cited 2024 Jan 8];186: S11–4.
22. Mytsyk Y, Dutka I, Yuriy B, Maksymovych I, Caprnda M, Gazdikova K, et al. Differential diagnosis of the small renal masses: role of the apparent diffusion coefficient of the diffusion-weighted MRI. Int Urol Nephrol. 2018;50(2):197–204.
23. Akin IB, Altay C, Güler E, Çamlidağ I, Harman M, Danaci M, et al. Discrimination of oncocytoma and chromophobe renal cell carcinoma using MRI. Diagn Interv Radiol. 2019; 25:5–13.
24. Shen L, Zhou L, Liu X, Yang X. Comparison of biexponential and monoexponential DWI in evaluation of Fuhrman grading of clear cell carcinoma. Diagn Interv Radiol.

2017; 23:100–5.

25. Hotker AM, Mazaheni Y, Wibmer A, Zheng J, Moskowitz CS, Tickoo SK, et al. Use of DWI in the differentiation of renal cortical tumours. AJR Am J Roentgenol. 2016; 206:100–5.
26. Bernard Rosner (2000), Fundamentals of Biostatistics, 5th Edition, Duxbury, page 80-240
27. Lassel EA, Rao R, Schwenke C, Schenberg SO, Michaely HJ. Diffusion weighted imaging of focal renal lesions: a meta-analysis. Eur Radiol. 2014; 24:241–9.
28. Muller MF, Prasad PV, Bimmler D, Kaiser A, Edelman RR. Functional imaging of the kidney by means of measurement of the apparent diffusion coefficient. Radiology 1994; 193:711–5.
29. Sun MR, Ngo L, Genega EM, et al. Renal cell carcinoma: dynamic contrast-enhanced MR imaging for differentiation of tumor subtypes—correlation with pathologic findings. Radiology 2009; 250:793–802
30. Ruppert-Kohlmayr AJ, Uggowitzer M, Meissnitzer T, Ruppert G. Differentiation of renal clear cell carcinoma and renal papillary carcinoma using quantitative CT enhancement parameters. AJR 2004; 183:1387–1391
31. Xu Y, Wang X, Jiang X. Relationship between the renal apparent diffusion coefficient and glomerular filtration rate: preliminary experience. J Magn Reson Imaging 2007; 26:678–681
32. Yildirim E, Gullu H, Caliskan M, Karadeli E, Kirbas I, Muderrisoglu H. The effect of hypertension on the apparent diffusion coefficient values of kidneys. Diagn Interv Radiol 2008; 14:9–13
33. Verswijvel G, Vandecaveye V, Gelin G, et al. Diffusion weighted MR imaging in the evaluation of renal infection: preliminary results. JBR-BTR 2002; 85:100–103

34. Chan JH, Tsui EY, Luk SH, et al. MR diffusion weighted imaging of kidney: differentiation between hydronephrosis and pyonephrosis. Clin Imaging 2001; 25:110–113
35. Nicolau, C.; Aldecoa, I.; Bunesch, L.; Mallofre, C.; Sebastia, C. The Role of Contrast Agents in the Diagnosis of Renal Diseases. Curr. Probl. Diagn. Radiol. 2015, 44, 346–359.
36. Kang, S.K.; Huang, W.C.; Pandharipande, P.V.; Chandarana, H. Solid renal masses: What the numbers tell us. AJR Am. J. Roentgenol. 2014, 202, 1196–1206.
37. Sasaguri, K.; Takahashi, N. CT and MR imaging for solid renal mass characterization. Eur. J. Radiol. 2018, 99, 40–54.
38. Lassel, E.A.; Rao, R.; Schwenke, C.; Schoenberg, S.O.; Michaely, H.J. Diffusion-weighted imaging of focal renal lesions: A meta-analysis. Eur. Radiol. 2014, 24, 241–249.
39. Zhong, J.; Cao, F.; Guan, X.; Chen, J.; DIng, Z.; Zhang, M. Renal cyst masses (Bosniak category II-III) may be over evaluated by the Bosniak criteria based on MR findings. Medicine 2017, 96, e9361.
40. Inci, E.; Hocaoglu, E.; Aydin, S.; Cimilli, T. Diffusion-weighted magnetic resonance imaging in evaluation of primary solid and cystic renal masses using the Bosniak classification. Eur. J. Radiol. 2012, 81, 815–820.
41. Balyemez, F.; Aslan, A.; Inan, I.; Ayaz, E.; Karagöz, V.; Özkanli, S.¸S.; Acar, M. Diffusion-weighted magnetic resonance imaging in cystic renal masses. Can. Urol Assoc. J. 2017, 11, E8–E14.
42. Wang, H.; Cheng, L.; Zhang, X.; Wang, D.; Guo, A.; Gao, Y.; Ye, H. Renal cell carcinoma: Diffusion-weighted MR imaging for subtype differentiation at 3.0 T.

Radiology 2010, 257, 135–143.

43. Kay, F.U.; Pedrosa, I. Imaging of Solid Renal Masses. Urol. Clin. N. Am. 2018, 45, 311–330.
44. Le Bihan D, Turner R, Douek P, et al. Diffusion MR imaging: clinical applications. Am J Roentgenol 1992; 159:591–599.
45. Rosenkrantz AB, Oei M, Babb JS, et al. Diffusion-weighted imaging of the abdomen at 3.0 Tesla: image quality and apparent diffusion coefficient reproducibility compared with 1.5 Tesla. J Magn Reson Imaging 2011; 33:128– 135.
46. Bilgili MYK. Reproducibility of apparent diffusion coefficient measurements in diffusion-weighted MRI of the abdomen with different b values. Eur J Radiol 2012;81: 2066–2068.
47. Maruyama M, Yoshizako T, Uchida K, et al. Comparison of utility of tumor size and apparent diffusion coefficient for differentiation of low- and high-grade clear-cell renal cell carcinoma. Acta Radiol 2015;56: 250–256.
48. Goyal A, Sharma R, Bhalla AS, et al. Pseudotumours in chronic kidney disease: can diffusion-weighted MRI rule out malignancy. Eur J Radiol 2013; 82:1870–1876.
49. SManenti G, Di Roma M, Mancino S, et al. Malignant renal neoplasms: correlation between ADC values and cellularity in diffusion weighted magnetic resonance imaging at 3 T. Radiol Med (Torino) 2008;113:199–213.
50. Manenti G, Di Roma M, Mancino S, et al. Malignant renal neoplasms: correlation between ADC values and cellularity in diffusion weighted magnetic resonance imaging at 3 T. Radiol Med (Torino) 2008;113:199–213.
51. Akita H, Jinzaki M, Akita A, et al. Renal cell carcinoma in patients with acquired cystic disease of the kidney: assessment using a combination of T2-weighted,

diffusion- weighted, and chemical-shift MRI without the use of contrast material. J Magn Reson Imaging 2014;39: 924–930.

52. Sasamori H, Saiki M, Suyama J, et al. Utility of apparent diffusion coefficients in the evaluation of solid renal tumors at 3T. Magn Reson Med Sci 2014;13:89–95.
53. Agnello F, Roy C, Bazille G, et al. Small solid renal masses: Characterization by diffusion-weighted MRI at 3 T. Clin Radiol 2013;68:301–308
54. Namimoto T, Yamashita Y, Sumi S, Tang Y, Takahashi M. Focal liver masses: characterization with diffusion-weighted echo-planar MR imaging. Radiology 1997; 204:739–744.
55. Bernard Rosner (2000), Fundamentals of Biostatistics, 5th Edition, Duxbury, page 80-240
56. Taouli B, Vilgrain V, Dumont E, Daire JL, Fan B, Menu Y. Evaluation of liver diffusion isotropy and characterization of focal hepatic lesions with two single-shot echo-planar MR imaging sequences: a prospective study in 66 patients. Radiology 2003;226: 71–78.
57. Kim T, Murakami T, Takahashi S, Hori M, Tsuda K, Nakamura H. Diffusion-weighted single-shot echoplanar MR imaging for liver disease. AJR Am J Roentgenol 1999;173: 393–398.
58. Namimoto T, Yamashita Y, Mitsuzaki K, Nakayama Y, Tang Y, Takahashi M. Measurement of the apparent diffusion coefficient in diffuse renal disease by diffusion-weighted echo-planar MR imaging. J Magn Reson Imaging 1999; 9:832–837.
59. Sureka B, Mittal M. Solid renal masses in adults. Indian Journal of Radiology and Imaging. 2016;26(4):429.
60. Mürtz P, Flacke S, Träber F, van den Brink JS, Gieseke J, Schild HH. Abdomen:

Diffusion-weighted MR Imaging with Pulse-triggered Single-Shot Sequences. Radiology. 2002 Jul;224(1):258–64.

61. Choy B, Nayar R, Lin X. Role of renal mass biopsy for diagnosis and management: Review of current trends and future directions. Cancer Cytopathology. 2023 Mar 27;
62. Thoeny HC, Zumstein D, Simon-Zoula S, Eisenberger U, Frederik De Keyzer, Hofmann L, et al. Functional Evaluation of Transplanted Kidneys with Diffusion-weighted and BOLD MR Imaging: Initial Experience. Radiology. 2006 Dec 1;241(3):812–21.
63. Agnihotri S, Kumar J, Jain M, Kapoor R, Mandhani A. Renal cell carcinoma in India demonstrates early age of onset & a late stage of presentation. The Indian journal of medical research 2014; 140(5):624–9.
64. Yoshikawa T, Kawamitsu H, Mitchell DG, Ohno Y, Ku Y, Seo Y, et al. ADC Measurement of Abdominal Organs and Lesions Using Parallel Imaging Technique. American Journal of Roentgenology. 2006 Dec;187(6):1521–30.
65. Lee E, Seon Hwa Lee, Ronit Agid, Bae J, Keller A, terBrugge KG. Preoperative Grading of Presumptive Low-Grade Astrocytomas on MR Imaging: Diagnostic Value of Minimum Apparent Diffusion Coefficient. American Journal of Neuroradiology. 2008 Nov 1;29(10):1872–7
66. Murakami R, Hirai T, Kitajima M, Fukuoka H, Toya R, Nakamura H, etal. Magnetic resonance imaging of pilocytic astrocytomas: usefulness of the minimum apparent diffusion coefficient (adc) value for differentiation from high-grade gliomas. Acta radiologica. 2008 May 1;49(4):462–7.
67. Huisman, T.A.G.M., Loenneker, T., Barta, G. *et al.* Quantitative diffusion tensor MR imaging of the brain: field strength related variance of apparent diffusion

coefficient (ADC) and fractional anisotropy (FA) scalars. *Eur Radiol* **16**, 1651–1658 (2006).

68. Kitis O, Altay H, Calli C, Yunten N, Akalin T, Yurtseven T. Minimum apparent diffusion coefficients in the evaluation of brain tumors. European Journal of Radiology. 2005 Sep;55(3):393–400.
69. Hiwatashi A, Kinoshita T, Moritani T, Wang HZ, Shrier DA, Numaguchi Y, etal. Hypointensity on Diffusion-Weighted MRI of the Brain Related to T2 Shortening and Susceptibility Effects. American Journal of Roentgenology. 2003 Dec;181(6):1705–9.
70. Atlas SW, DuBois P, Singer MB, Lu D. Diffusion measurements in intracranial hematomas: implications for MR imaging of acute stroke. AJNR Am J Neuroradiol. 2000 Aug;21(7):1190-4. PMID: 10954267; PMCID: PMC8174893.
71. Pallagani L, Choudhary GR, Himanshu P, Madduri VKS, Singh M, Gupta P, etal. Epidemiology and Clinicopathological Profile of Renal Cell Carcinoma: A Review from Tertiary Care Referral Centre. Journal of kidney cancer and VHL [Internet]. 2021 [cited 2022 Dec 22];8(1):1–6.

ANNEXURES – I

ANNEXURE – I –CONSENT FORM

TITLE OF THE STUDY: "ROLE OF DIFFUSION-WEIGHTED MAGNETIC RESONANCE IMAGING IN THE EVALUATION OF RENAL MASSES: ONE YEAR HOSPITAL BASED OBSERVATIONAL STUDY"

NAME OF STUDENT/PRINCIPAL INVESTIGATOR: REG NO. BS0121002

OBJECTIVE: The study aims to assess the value of Diffusion-Weighted Magnetic Resonance Imaging in differentiating among the various subgroups of renal masses.

INTRODUCTION: Diffusion-weighted Weighted Imaging holds great potential for abdominal imaging, in particular for focal lesion detection, characterisation, and the evaluation of diffuse parenchymal diseases.

The study aids in early detection and differentiation of renal masses through a noninvasive MRI DWI sequence.

EXPLANATION OF PROCEDURE: I request you to kindly participate in the study titled study **"ROLE OF DIFFUSION-WEIGHTED MAGNETIC RESONANCE IMAGING IN THE EVALUATION OF RENAL MASSES: ONE YEAR HOSPITAL BASED OBSERVATIONAL STUDY"** at Dr Prabhakar Kore Hospital and Medical Research Centre, Belagavi is being conducted by REG NO. BS0121002, Postgraduate in Radio diagnosis at J.N. Medical College, Belagavi, Karnataka, under the guidance of _____., Dept. of Radio-diagnosis, J. N. Medical College, Belagavi.

We request you to participate in this study as you are eligible to be included. During the survey, you will be asked questions regarding your present and past medical history and required to answer to the best of your knowledge. You will also be clinically examined as per the protocol drawn.

If you agree to participate in the study, please furnish the details about the study.

BENEFITS: No use of surgical equipment /risk associated with it.

ALTERNATIVES: If you are not willing to take part in the study, your treatment or any other further investigations the patient wants to undergo, in the future, in KLE will not be affected by your decision.

WITHDRAWAL FROM PARTICIPATION IN THE STUDY: Participation in this study is voluntary. You can decide whether to participate in this study or continue participation once enrolled. In case you decide to withdraw your participation, you are free to do so. However, please convey the decision to the principal investigator.

POSSIBLE BENEFITS FROM PARTICIPATING IN THE STUDY: You will/will not have nor get any benefits by participating in this study. The data gathered will help the population at large.

POSSIBLE RISKS FROM PARTICIPATING IN THE STUDY: There are no risks involved in participating in this study.

PRIVACY AND CONFIDENTIALITY: The information collected from you will be coded to prevent any person from identifying you. Your identity will never be

revealed. The data collected from you will be kept confidential, and only processed or aggregated data will be used for publication.

COSTS: NIL (The study is to be conducted on the participants who are advised for MRI as an investigation by the referring consultant and the participants will not bear the charges for it).

FINANCIAL INCENTIVES: You will not receive any payment for participating in this study.

AUTHORISATION FOR PUBLICATION OF AGGREGATED DATA: Results obtained after processing of the aggregated data will be published for scientific purposes and or presented to scientific groups. However, your identity will never be revealed.

QUESTIONS: In case of any questions about this study, you are free to contact:

REG NO. BS0121002	**DR. _____**	**DR. HARSHA HEGDE,**
Post-Graduate, Department of Radio-Diagnosis. J.N. Medical College, Belagavi	Guide, Professor, Department of Radio-Diagnosis J.N. Medical College, Belagavi	CHAIRPERSON, JNMC, IEC & SCIENTIST D, ICMR, NATIONAL INSTITUTE OF TRADITIONAL MEDICINE, BELAGAVI

LEGAL RIGHTS: By signing this consent form, we are not waiving any of your legal rights.

CONSENT STATEMENT

I am making a voluntary decision to participate in the study **"ROLE OF DIFFUSION-WEIGHTED MAGNETIC RESONANCE IMAGING IN THE EVALUATION OF RENAL MASSES: ONE YEAR HOSPITAL BASED OBSERVATIONAL STUDY".** My signature below indicates that I have decided to participate, and I have read the information provided above, or the information provided above has been read to me in the language that I understand best. I was given the opportunity to ask questions, which were answered to my satisfaction.

Name of the participant: _____

A signature or left thumb impression of the participant:

Name of the witness: _____

Signature or left thumb impression of the witness:

Name of the investigator: _____

Signature of the investigator:

ANNEXURE – II – PROFORMA

ROLE OF DIFFUSION-WEIGHTED MAGNETIC RESONANCE IMAGING IN THE EVALUATION OF RENAL MASSES: ONE YEAR HOSPITAL-BASED OBSERVATIONAL STUDY

Patient identification number:

Name:

Age:

Sex:

Occupation:

Referred by: Self/ Physician

Address:

Contact number:

Presenting complaints:

Symptoms	**Present**	**Absent**	**If present, then the Duration of the illness**
Abdominal pain			
Abdominal distension			
Fever			
Nausea			
Vomiting			
Hematuria			
Burning micturition			
Urinary incontinence			
Loss of appetite			
History of weight loss			
Lower limb swelling			

Past medical history:

Hypertension ☐ Diabetes ☐ Asthma ☐ Ischemic ☐ disease

H/o TB ☐ H/o Allergies ☐ (please specify):-

Past surgical history:

Menstrual history:

Family history:

MRI findings:

Kidney affected: **Right** ☐ **Left** ☐ **Both** ☐

Nature of lesion (mention number of lesions in box)**:**

Solid: Right side ☐ **Cystic:** Right side ☐

Complex-cystic: Right side ☐

Left side ☐ Left side ☐ Left side ☐

Lesion under evaluation:

CATEGORY	**FINDINGS**
ON ROUTINE MRI SEQUENCES	**T1W:** **T2W:**
ON DWI: ➢ **DIFFUSION RESTIRCTION** ➢ **ADC VALUE:**	
MISCELLANEOUS **(if anything, please specify)**	

Lesion under evaluation:

CATEGORY	**FINDINGS**
ON ROUTINE MRI SEQUENCES	**T1W:** **T2W:**
<u>ON DWI:</u> ➢ **DIFFUSION RESTIRCTION** ➢ **ADC VALUE:**	
MISCELLANEOUS **(if anything, please specify)**	

Lesion under evaluation:

CATEGORY	**FINDINGS**
ON ROUTINE MRI SEQUENCES	**T1W:** **T2W:**
<u>ON DWI:</u> ➢ **DIFFUSION RESTIRCTION** ➢ **ADC VALUE:**	
MISCELLANEOUS **(if anything, please specify)**	

ANNEXURE – III – PHOTOGRAPHS

PHOTOGRAPH OF CASES

Case 1: A 72-year-old female with complaints of abdominal pain for the past two months.

A well-defined T2 isointense exophytic solid mass lesion with a few tiny cystic areas, measuring 3.0 (AP) x 2.4 (ML) x 2.3 (CC) cm, is present in the upper pole of the right kidney and shows restricted diffusion on the DWI sequence. HPR showed features of clear cell renal cell carcinoma.

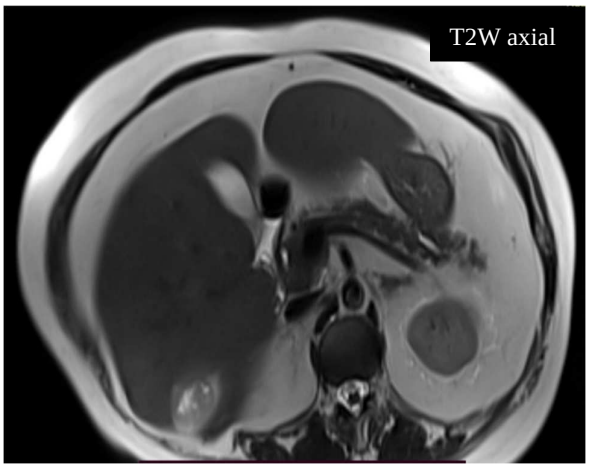

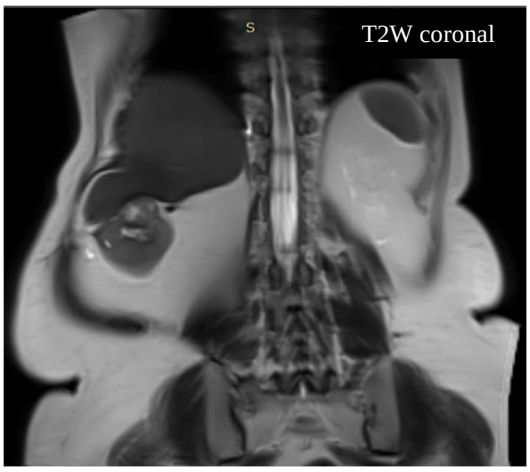

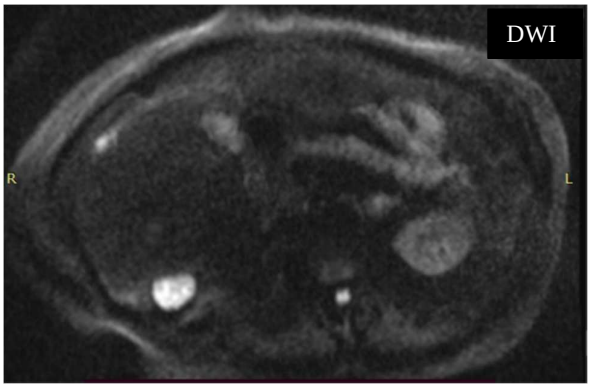

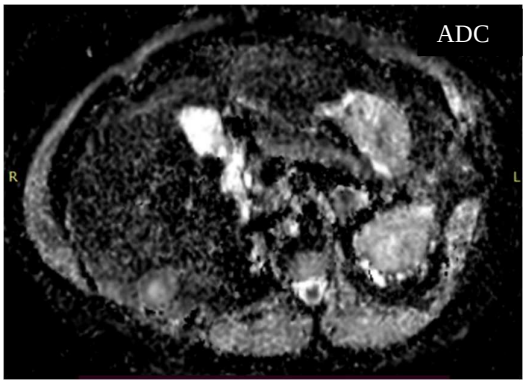

Case 2: A 56-year-old male with complaints of abdominal pain, haematuria, loss of appetite and weight for four months.

The left kidney shows a moderate degree of dilatation of the pelvicalyceal system due to a well-defined T2 hypointense solid mass lesion measuring 7.5 x 4.7 cm in the pelvicalyceal system, which shows restricted diffusion on the DWI sequence. HPR suggests features of transitional cell carcinoma.

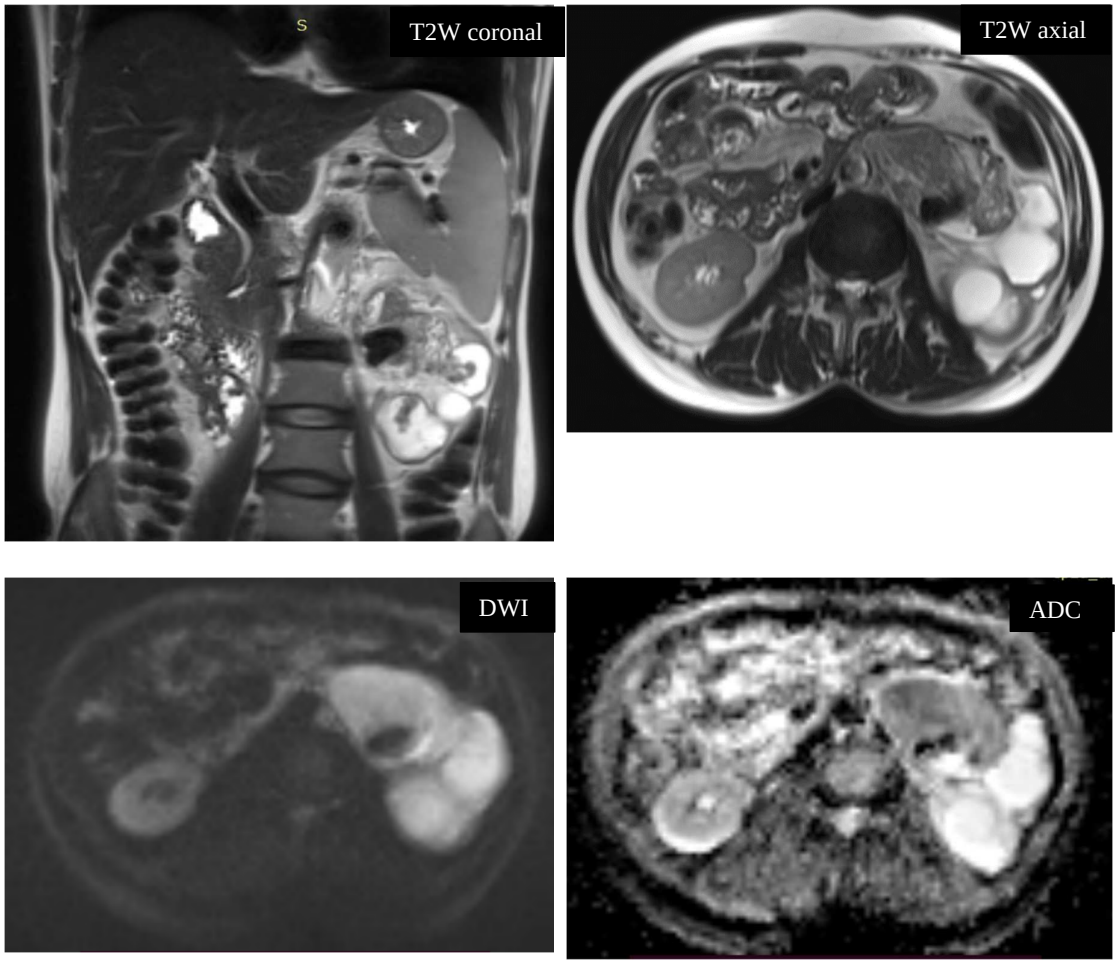

Case 3: A 75-year-old male with complaints of abdominal pain, haematuria, loss of appetite and weight for six months.

A large, well-defined T2 isointense exophytic solid mass lesion with internal hyperintensities measuring 9.1 (AP) x 8.3 (ML) x 8.3 (CC) cm involving the lower pole of the left kidney shows restricted diffusion on the DWI sequence. HPR suggests features of chromophobe-type renal cell carcinoma.

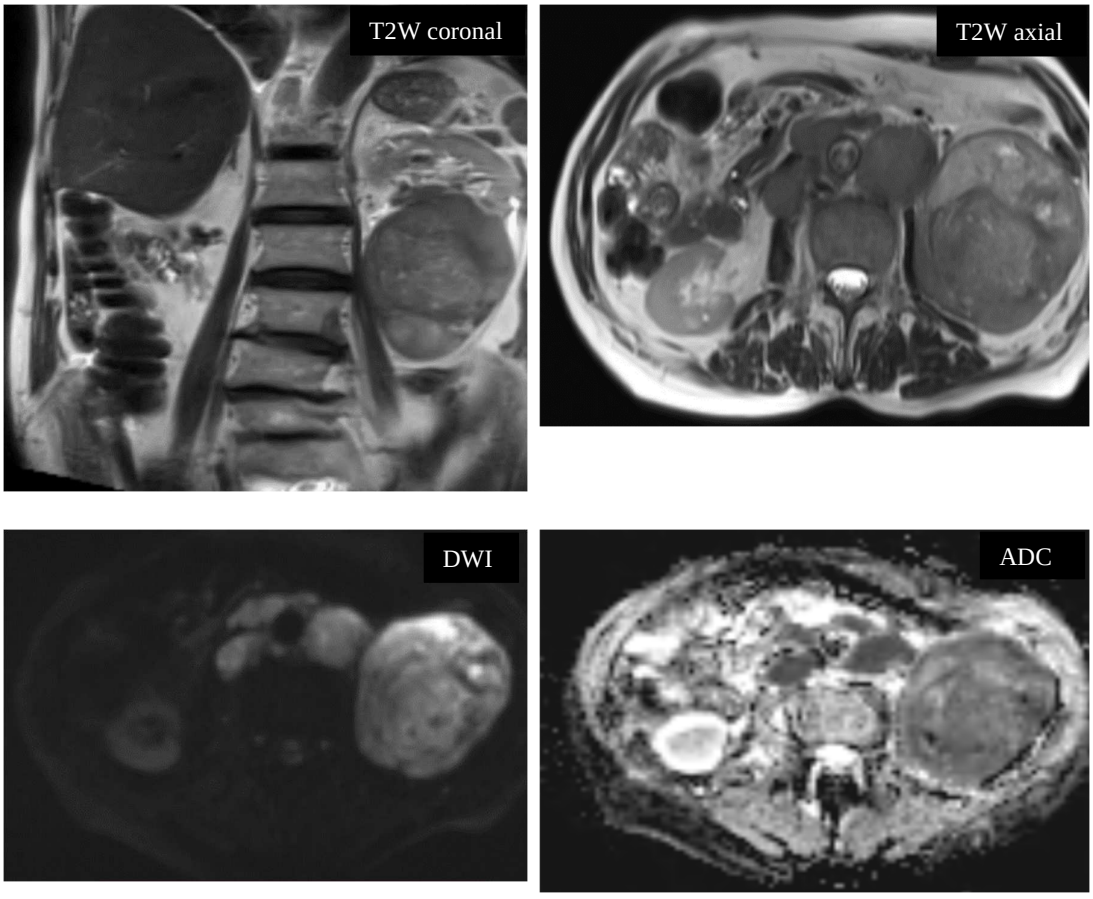

Case 4: A 53-year-old male with complaints of abdominal pain, haematuria, urinary incontinence, loss of appetite and weight for four months.

A well-defined T2 hypointense solid mass lesion measuring 4.5 (AP) x 3.6 (ML) x 3.1 (CC) cm in the mid-pole of the right kidney shows restricted diffusion on the DWI sequence. HPR suggests features of papillary-type renal cell carcinoma.

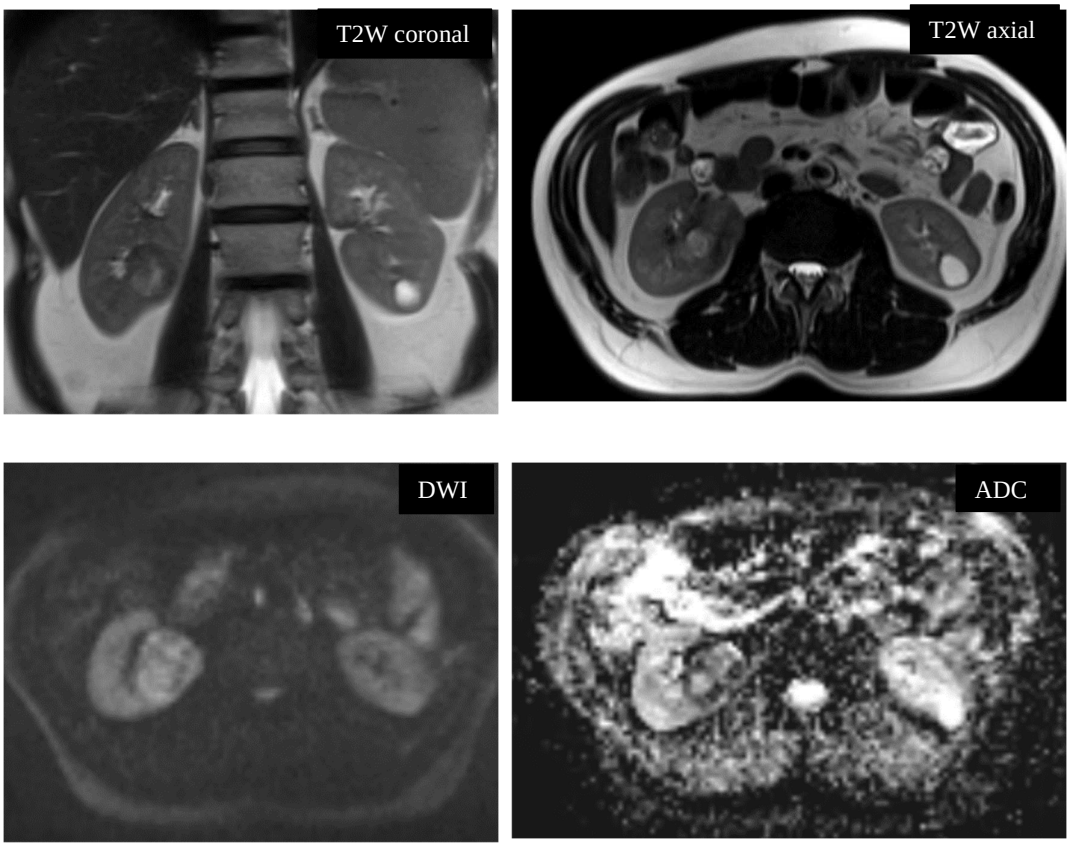

Case 5: A 53-year-old male with complaints of abdominal pain, haematuria, urinary incontinence, loss of appetite and weight for four months.

A large ill-defined exophytic T2 hyperintense solid mass lesion with internal areas of necrosis & haemorrhage measuring 12.5 (AP) x 11.2 (ML) x 15.7 (CC) cm noted arising from the upper pole of the right kidney shows areas of restricted diffusion on the DWI sequence. HPR suggests features of Wilms tumour.

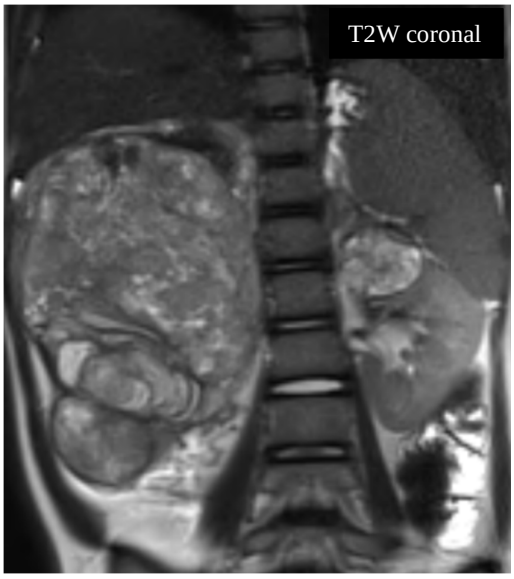

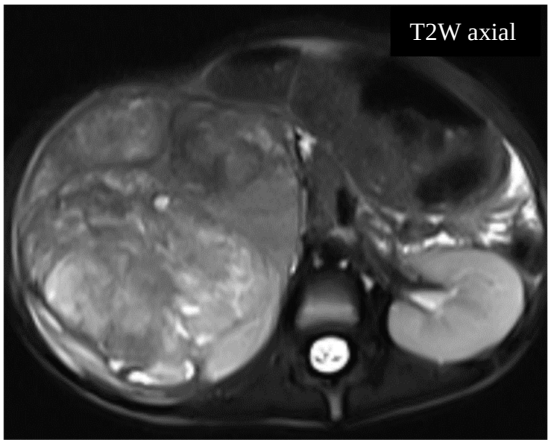

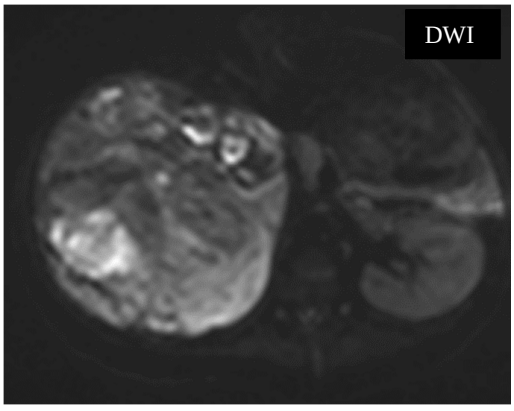

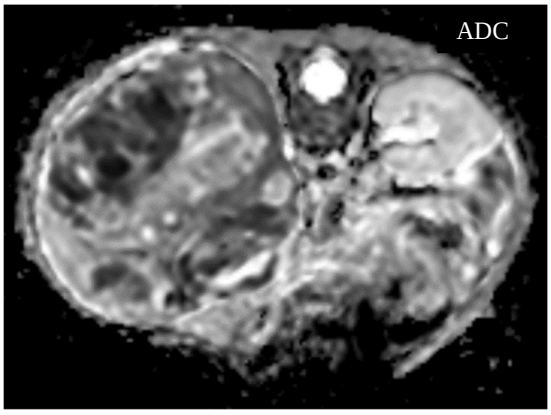

Case 6: A 62-year-old male patient complained of hematuria, burning micturition and urinary incontinence for the past month.

Large well-defined thin-walled cystic lesion with few internal septations and one thick internal septation noted in the lower pole of the right kidney, measuring 7.1 (AP) x 7.8 (ML) x 8.6 (CC) cm with no evidence of restricted diffusion on the DWI sequence. Features suggestive of Bosniak type III cyst.

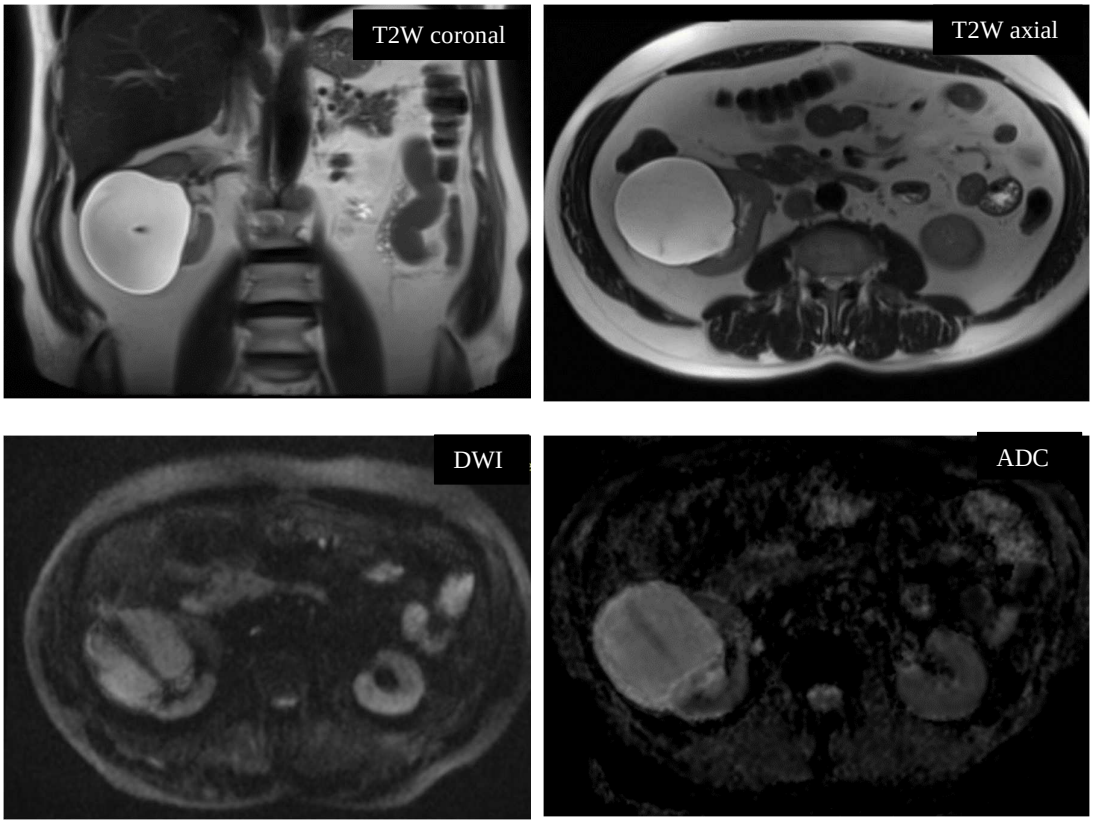

ANNEXURE – IV – KEY TO MASTERCHART

MALE	**M**
FEMALE	**F**

Abdominal pain	**1**
Abdominal distension	**2**
Fever	**3**
Nausea	**4**
Vomiting	**5**
Hematuria	**6**
Burning micturition	**7**
Urinary incontinence	**8**
Loss of appetite	**9**
History of weight loss	**10**
Lower limb swelling	**11**

PRESENT	**P**
ABSENT	**A**

RIGHT SIDE	**R**
LEFT SIDE	**L**
BOTH	**B**

YES	**Y**
NO	**N**

HYPOINTENSE	**HYPO**
HYPERINTENSE	**HYPER**
ISOINTENSE	**ISO**
HYPOINTENSE TO ISOINTENSE	**HI**
ISOINTENSE TO HYPERINTENSE	**IH**

DIFFUSION RESTRICTION	**DR**
ADC VALUES (x 10^{-3} mm^2/sec)	**ADC**

FEW THIN SEPTATIONS	**FTS**
MULTIPLE THIN SEPTATIONS	**MTS**
ONE THICK SEPTATION	**OTS**
THICK IRREGULAR SEPTATION	**TIS**

BOSNIAK TYPE I CYST	**B.I**
BOSNIAK TYPE II CYST	**B.II**
BOSNIAK TYPE IIF CYST	**B.IIF**
BOSNIAK TYPE III CYST	**B.III**
BOSNIAK TYPE IV CYST	**B.IV**

Clear cell RCC	**ccRCC**
Chromophobe Type RCC	**chRCC**
Papillary Type RCC	**pRCC**
Transitional cell carcinoma	**TCC**
Wilms tumour	**Wilms**

Master Chart

PT S.NO	AGE(yrs)	SEX	SYMPTOMS	CO-MORBIDITIES	SIDE AFFECTED	S.NO OF LESION	size <4cm	size 4-8 cm	size >8 cm	SOLID LESION	CYSTIC LESION	COMPLEX CYSTIC	T1W	T2W	NECROSIS	SEPTATIONS	DR	ADC	benign lesions	malignant lesions
1	72	F	1	P	R	1	Y			Y			HYPO	ISO	P	A	P	2.325		ccRCC
2	46	M	1, 6, 7, 9, 10	P	L	2		Y		Y			HYPER	IH	P	A	P	1.429		ccRCC
3	51	M	1, 7	P	B	3		Y			Y		HYPO	HYPER	A	A	A	2.546	B.I	
						4		Y			Y		HYPO	HYPER	A	A	A	3.001	B.I	
						5	Y				Y		HYPO	HYPER	A	A	A	2.952	B.I	
4	73	M	nil	P	B	6	Y				Y		HYPO	HYPER	A	A	A	3.087	B.I	
						7	Y				Y		HYPO	HYPER	A	A	A	2.613	B.I	
						8	Y				Y		HYPO	HYPER	A	A	A	2.978	B.I	
5	62	M	7, 6, 8	P	R	9			Y		Y		HYPO	HYPER	A	OTS	A	3.457	B.III	
6	56	M	1, 6, 7 9 10	P	L	10		Y		Y			HYPO	HYPO	A	A	P	1.226		TCC
7	23	M	1, 9	A	R	11	Y				Y		HYPO	HYPER	A	FTS	A	3.017	B.II	
						12	Y					Y	ISO	HYPER	A	A	P	2.105	B.IV	
8	51	F	1, 7	P	L	13	Y				Y		HYPO	HYPER	A	A	P	2.487	B.I	
9	43	M	1, 6, 7, 9, 10	P	R	14		Y		Y			HI	IH	P	A	P	2.199		ccRCC
10	58	M	nil	P	B	15	Y				Y		HYPO	HYPER	A	A	A	3.476	B.I	
						16		Y			Y		HYPO	HYPER	A	A	A	3.241	B.I	
11	65	F	1, 6	P	B	17		Y		Y			ISO	IH	P	A	P	2.107		ccRCC
						18	Y				Y		HYPO	HYPER	A	A	A	3.792	B.I	
12	38	F	1, 6	A	R	19	Y			Y			ISO	ISO	A	A	P	2.125		ccRCC
13	69	M	1	P	L	20	Y				Y		HYPO	HYPER	A	A	A	2.977	B.I	
14	53	M	1, 6, 8, 9, 10	P	B	21		Y		Y			HYPO	HYPO	A	A	P	1.192		pRCC
						22	Y				Y		HYPO	HYPER	A	A	A	3.312	B.I	
15	40	F	1, 7, 8	P	L	23	Y			Y			HYPER	HYPO	A	A	A	1.075		chRCC
16	59	F	nil	P	L	24	Y				Y		HYPO	HYPER	A	A	A	3.025	B.I	
17	58	M	nil	P	R	25	Y				Y		HYPO	HYPER	A	A	A	3.089	B.I	
18	75	M	1, 6,9, 10	P	L	26			Y	Y			ISO	IH	A	A	P	1.031		chRCC
19	56	F	8	P	R	27	Y				Y		HYPO	HYPER	A	A	A	2.933	B.I	
20	49	M	1, 6, 7, 9, 10	P	L	28			Y	Y			HYPO	IH	P	A	P	1.638		ccRCC
						29	Y			Y			ISO	ISO	P	A	P	1.465		ccRCC
21	55	F	4, 5	P	L	30	Y				Y		HYPO	HYPER	A	FTS	A	2.882	B.II	
22	64	F	1, 6, 7, 10	P	B	31		Y		Y			HYPO	HYPER	P	A	P	1.587		ccRCC
						32	Y						HYPO	HYPER	A	A	A	2.887	B.I	
23	37	F	6, 7, 9, 10	A	R	33	Y			Y			ISO	ISO	A	A	P	0.631		chRCC
24	59	M	nil	P	L	34	Y				Y		HYPO	HYPER	A	A	A	3.481	B.I	
25	68	M	1	P	R	35	Y				Y		HYPO	HYPER	A	A	A	3.121	B.I	
26	35	M	1, 6	P	R	36		Y		Y			HYPO	HYPER	P	A	P	1.679		ccRCC
						37	Y			Y			HYPO	HYPER	A	A	P	1.597		ccRCC
27	51	M	1	P	L	38	Y				Y		HYPO	HYPER	A	FTS	A	2.787	B.II	
28	12	F	1	A	R	39			Y	Y			HYPO	HYPER	P	A	P	0.789		Wilms
29	60	F	nil	P	B	40			Y		Y		HYPO	HYPER	A	FTS	P	3.043	B.II	
						41	Y				Y		HYPER	IH	A	A	P	2.936	B.II	
30	64	M	1	A		42		Y			Y		HYPO	HYPER	A	MTS	A	2.937	B.II	
						43	Y				Y		HYPO	HYPER	A	A	A	3.261	B.I	
						44	Y				Y		HYPO	HYPER	A	A	A	3.367	B.I	
31	5	F	1, 2	A	R	45			Y	Y	Y		HYPO	HYPER	A	A	P	0.767		Wilms
32	56	M	nil	P	R	46	Y				Y		HYPO	HYPER	A	FTS	A	3.126	B.II	

33	59	M	nil	P	L	47	Y						HYPO	HYPER	A	A	A	3.287	B.I	
34	7	F	1, 2	A	L	48			Y			Y	HYPO	HYPER	A	A	P	0.761		Wilms
35	77	M	1, 6, 10	P	R	49		Y		Y			HYPO	HYPER	P	A	P	1.787		ccRCC
36	56	M	1	P	L	50		Y			Y		HYPO	HYPER	A	TIS	A	2.987	B.II	
37	47	F	1, 6, 9, 10	A	R	51		Y		Y			HI	ISO	A	A	P	1.107		pRCC
38	4	M	1, 2	A	L	52			Y	Y			HYPO	IH	A	A	P	0.789		Wilms
39	66	M	1	P	L	53		Y			Y		HYPO	HYPER	A	A	A	3.617	B.I	
40	3	M	1, 2	A	L	54			Y	Y			ISO	HYPER	A	A	P	0.713		Wilms
41	56	M	nil	A	R	55	Y				Y		HYPO	HYPER	A	A	A	3.248	B.I	
42	46	F	nil	A	L	56	Y				Y		HYPO	HYPER	A	A	A	3.158	B.I	
43	38	M	1	A	R	57	Y				Y		HYPO	HYPER	A	A	A	3.354	B.I	
44	64	F	nil	A	R	58	Y				Y		HYPO	HYPER	A	A	A	3.568	B.I	